of GBM (1). The long arm of chromosome 13 is lost in nearly 33% to 50% of these tumors; the *Rb* gene is at least one of the targets in this deletion, being inactivated in ~35% of samples (5-8). Loss of chromosomal material on chromosome 10 occurs in 60% to 95% of GBMs (9). One common minimum deleted region (CMDR) at 10q23.3 includes the *PTEN* gene, which occurs in approximately 20% to 30% of samples (10-12). Epidermal growth factor receptor (*EGFR*) is amplified in ~40% of GBMs (9). Of interest, 33% of these tumors with *EGFR* amplification have a specific *EGFR* rearrangement, producing a smaller protein, making it similar to the *v-erbB* oncogene (13). Amplification of *EGFR* is associated with overexpression of the EGFR protein and it is often associated with deletion of *PTEN* and *p16(INK4A)* (14). Alterations of chromosome 17p are associated with a mutation of the *p53* gene in ~30% of GBMs. The prominent vascularity that occurs in GBM is probably the result of excess expression of growth factors and their receptors [e.g., vascular growth factor receptor (VEGFR) and platelet-derived growth factor receptor (PDGFR)] that are associated with angiogenesis.

We used high-density (50K/250K) arrayed oligonucleotide probes that contain single nucleotide polymorphisms (SNP), the so-called SNP-Chip, to identify genetic abnormalities, including amplicons, duplications, deletions, and acquired uniparental disomy [AUPD; loss of heterozygosity (LOH) with normal copy number]. Our SNP-Chip results were validated using several other techniques, including quantitative PCR (Q-PCR), nucleotide sequencing, and detection of LOH by microsatellite markers. Using SNP-Chips, we identified aberrant genes as well as aberrant genetic pathways in GBM. This robust technology should set the stage to formulate new diagnostic subcategorizations of GBM and to provide prognostic indicators for physicians to set up personalized therapy according to the aberrant genetic pattern of the GBM of the individual.

Results

Signaling Pathway Abnormalities Present in GBM

DNA from 55 GBMs (22 with matched normal peripheral blood neutrophils) and 6 GBM cell lines were examined by SNP-Chip assay for genomic abnormalities (Tables 1 and 2). Common duplications and deletions of either segments or entire chromosomes were observed. For example, chromosome 7 was duplicated in 30 of 55 GBM samples, and deletion of either all or part of chromosome 10 occurred in 33 of 55 GBM samples. Also, small common minimally deleted regions (CMDR) or small common minimally amplified regions (CMAR) that involved only one or several genes were found. For example, 36 of 55 clinical samples had a deletion at chromosome 9p21.3 containing the *p14(ARF)*, *p15(INK4B)*, and *p16(INK4A)* tumor suppressor genes (Fig. 1A); notably, 20 of these 36 GBM samples had homozygous deletions at this site. Also, 36 of 55 samples had either duplication (19 samples) or amplification (17 samples) at chromosome 7p11.2, which contained the *EGFR* gene (Fig. 1C; five representative samples). The CMDRs and CMARs were confirmed by reverse transcription Q-PCR (Fig. 1B and D). All the CMDRs and CMARs are summarized on Table 1. For 51 of the 55 GBM patients, survival data were available. Median survival time was 60 weeks. Overall, 39 events were reported. Significant short survival time (*P* values were not corrected for multiple testing) was found in the patients with 13q14 (*RB*) deletion (Fig. 1E) or 17p13.1 (*p53*) deletion/AUPD (Fig. 1F). In these CMDR and CMAR, the genes involve in the p16(INK4A)/p15(INK4B)-CDK4/6-pRb (pathway 1) and the p14(ARF)-MDM2/4-p53 (pathway 2) were frequently aberrant: pathway 1 had deletion of *p16(INK4A)* and *p15 (INK4B)* in 66% of cases; deletion of *Rb* in 40% of cases; and amplification of *CDK4* in 11% and trisomy of *CDK6* in 55%. Pathway 2 had deletion of *p14(ARF)* in 66% cases, deletion or AUPD of p53 in 33%, and amplification of *MDM2* in 11% and trisomy or amplification of *MDM4* in 13%. Alteration of *MDM2* and *MDM4* was mutually exclusive in the same sample. Taken together, alterations of p16 (INK4A)/p15(INK4B)-CDK4/6-pRb pathway occurred in 48 of 55 (87%) cases, and the p14(ARF)-MDM2/4-p53 pathway was abnormal in 48 of 55 (87%) samples; both pathways were simultaneously aberrant in 46 of 55 (84%) cases. In addition, the pathway associated with tyrosine kinase receptor signaling (pathway 3), including deletion of *PTEN* or amplification of *EGFR* and/or *VEGFR/PDGFR* α (*PDGFRA*), was detected in 39 of 55 GBM samples (71%).

SNP-Chip array of chromosome 2 from the U118 GBM cell line showed a deletion in the *LRP1B* gene, spanning exons 3 to 18 (Fig. 2). Nucleotide sequencing of the cDNA of *LRP1B* showed a truncated LRP1B in which exons 2 and 19 were fused

Table 1. Common Minimal Region of Deletion, Amplification, and Acquired Uniparental Disomy

Minimal Region	No. Affected Samples (%)	Selected Genes Within the Region
CMDR		
1p36.23 (1,720 kb)	19/55 (35%), 16 D and 3 DD	*CAMTA1, PER3, UTS2, TNFSF9, VAMP3, PARK7, MIG6, RERE, GPR157, H6PD*
2q22.1 (479 kb)	4/55 (7%), 4D	*LRP1B*
6q 26-27 (3,133 kb)	16/55 (29%), 14 D and 2 DD	*PARK2, PACRG, QKI, PDE10A*
9p21.3 (981 kb)	36/55 (66%), 16 D and 20 DD	*p14(ARF), p15(INK4B), p16(INK4A)*
10q23.31 (693 kb)	33/55 (60%), 31 D and 2 DD	*PTEN*
13q14.2-14.3 (1,987 kb)	22/55 (40%), 21 D and 1 DD	*Rb, KCNRG*
17p 13.1 (636 kb)	10/55 (18%), 10 D	*p53*
CMAR		
1q32.1 (758 kb)	7/55 (13%), 4A and 3 AA	*MDM4, NFASC, LRRN5*
4q11-12 (3,157 kb)	5/55 (9%), 2 A and 3 AA	*PDGFRA, KIT, VEGFR, CLOCK*
7p11.2 (660 kb)	36/55 (66%). 19 A and 17 AA	*EGFR*
12q14.1 (390 kb)	6/55 (11%), 6 AA	*CDK4*
12q15 (795 kb)	6/55 (11%), 6 AA	*MDM2*
AUPD		
17p 13.3-12 (10,700 kb)	8/55 (15%)	*p53*

NOTE: D, heterozygous deletion; DD, homozygous deletion; A, trisomy; AA, high-level copy number amplifications.

and an early stop codon occurred, resulting in only a 75-amino-acid open reading frame. Internal deletion of *LRP1B* also occurred in four GBM samples (representative samples shown in Fig. 2). The results suggest that internal deletion of *LRP1B* is associated with development of glioma. We also found that one sample had marked amplification of chromosome 5p13.2 (Fig. 3A). About 20 genes are localized in this amplicon, including *IL7R, CAPSL, SKP2*, and *SLC1A3*. *SKP2* is required for ubiquitin-mediated degradation of the CDK inhibitor p27 (KIP1). We measured mRNA levels of *SKP2* in 21 GBM tumor samples and 6 normal brain samples; the gene was highly expressed in 52% (11 of 21) of the GBM samples (>2-fold the average level of six normal brain samples; Fig. 3B).

Deletion at 1p36.23 and 6q26-27 in GBM

A total of 19 of 55 GBM samples had a deletion that included 1p36.23; 11 had a small heterozygous and 3 had a homozygous deletion at this region involving two CMDRs (Fig. 4). Genes within these CMDRs include *CAMTA1, PER3, UTS2, TNFSF9, VAMP3, PARK7, MIG6, RERE* in one region, and

Table 2. Summary of Genomic Abnormality in Clinical Samples

Case	Sex	Age	Surv (wk)	Status	1p36 Del	1q32.1 Amp (*MDM4*)	4q11-12 Amp (*VEGF*)	6q26-27 Del	7p11.2 Amp (*EGFR*)	9p21.3 Del (*p14, p15, p16*)	10q23 Del (*PTEN*)	12q14.1 Amp (*CDK4*)	12q115 Amp (*MDM2*)	13q14 Del (*RB*)	17p13.1 Del/AUPD (*p53*)
S1	M	45	48	D			++		+	++	+			+	AUPD
S2	M	56	39	D					+		+			+	AUPD
S3	F	56	30	D				+	++	++	+				
S4	M	49	60	D					++	++	+				
S5	F	56	56	D			++	+	++	++	+				
S6	M	47	51	D	++				++	++	+				
S7	F	57	60	D				++	+	++	+			+	
S8	M	55	64	D					+	++	+				
S9	M	65	51	D					+				++	++	AUPD
S10	M	64	26	D	+			++	++	++	++				
S11	M	46	64	D											
L2	M	48	86	D											
L3	F	43	180	D	+			+		+					
L4	F	42	300	A	+					++					
L5	M	56	99	D					+	++	+				
L6	M	63	291	A		+	+	+	++	+	+	++			
L7	F	39	360	A				+	++	+	+				
L10	F	49	111	D			++		+	++	+				
G1	F	NA	NA	NA					+	++	+		++	+	
G7	F	NA	NA	NA			+	+	+	+	+	++		+	AUPD
G5	F	NA	NA	NA					+	+	+				+
G12	F	NA	NA	NA				+	+	+					AUPD
C3	F	63	18	A		++			++						
C4	M	37	23	A	+					+					
C5	M	65	25	A				+	++	++	+				
C6	M	70	3	D	+			+	++	++	+			+	
C7	M	50	5	D											
C8	M	46	79	D		++			++	++	+				+
C9	M	59	39	A		+									
C10	M	26	16	A						+					
C11	F	63	18	A		++			++	++	+			+	
C12	M	48	20	A	++						+			+	+
C13	M	24	115	A											
C14	F	39	58	D											
C15	F	76	8	D	+	++			+	AUPD	+			+	AUPD
C18	M	18	11	D						+					AUPD
C19	F	56	75	D	++				+	++	++			+	
C20	M	49	201	D					+						
C21	M	65	40	D	+				+		AUPD	++	++		+
C22	M	48	20	A	+				+	+	+			+	
D1	M	66	25	D	+			+	++	++	+			+	
D2	M	57	22	D	+					++	+				+
D3	F	54	8	D											
D4	M	50	48	D	+									+	+
D5	F	60	65	D	+			+	++	++	+			+	+
D6	M	42	99	D		+								+	
D7	F	61	49	D					+		+	++	++	+	
D8	F	69	165	D					++	+	+	++	++	+	
D9	F	64	42	D	+				++			++	++		
D10	M	66	22	D	+				+	+				+	
D11	F	42	99	D					++	++	+				
D12	M	39	95	D	+			+		+					+
D13	M	20	86	D				+						+	AUPD
D14	F	50	17	D	+				+		+			+	+
D15	M	30	38	D				+		+	+			+	+

NOTE: Status: D, dead; A, alive; Surv, survival from time of first surgery: ++, homozygous deletions or high-level copy number amplifications; +, hemizygous deletion or trisomy; Amp, amplification; Del, deletion. Candidate genes are provided in parentheses.

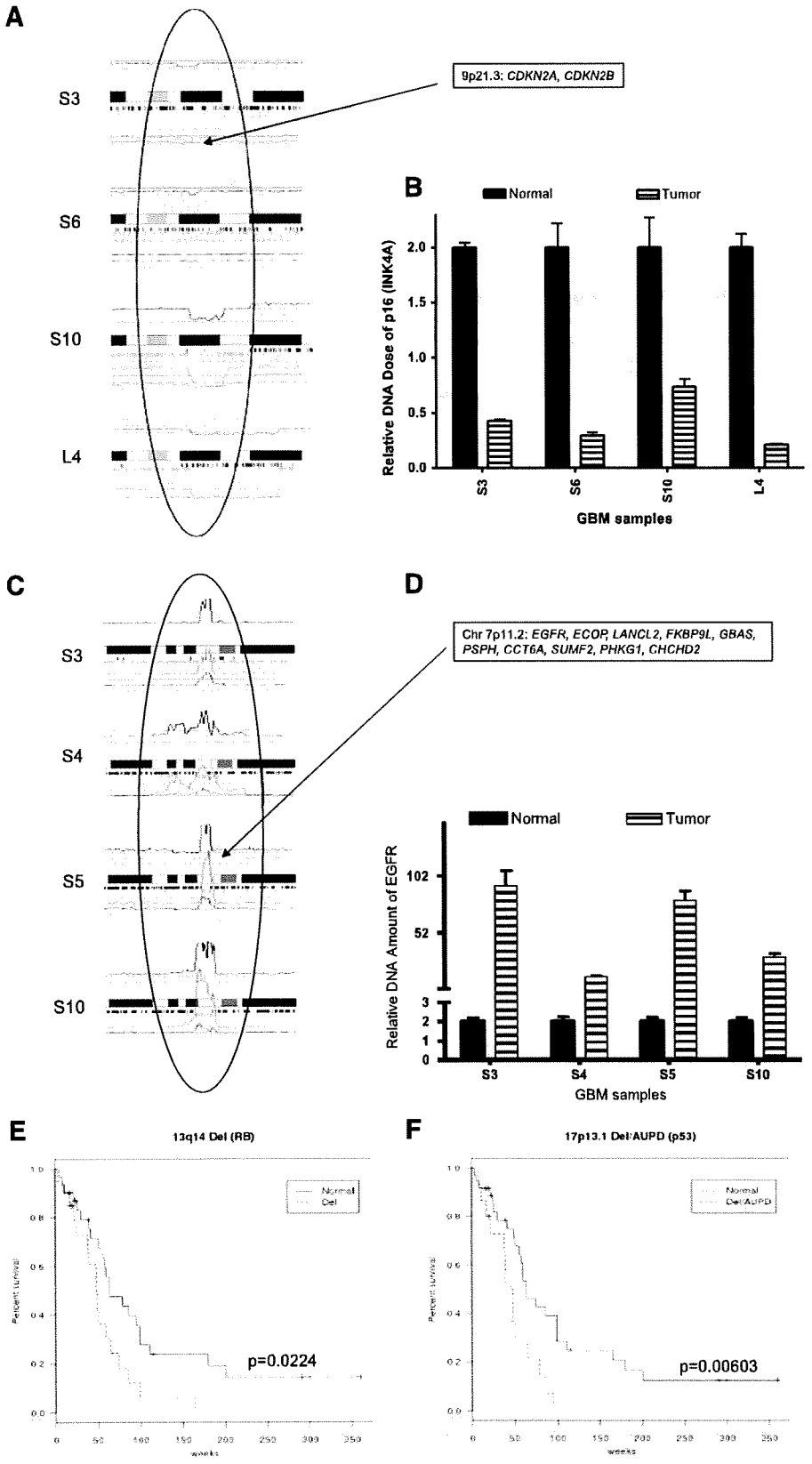
A
S3
S6
S10
L4
9p21.3: CDKN2A, CDKN2B
B
Normal
Tumor
Relative DNA Dose of p16 (INK4A)
2.0
1.5
1.0
0.5
0.0
S3
S6
S10
L4
GBM samples
C
S3
S4
S5
S10
D
Chr 7p11.2: EGFR, ECOP, LANCL2, FKBP9L, GBAS, PSPH, CCT6A, SUMF2, PHKG1, CHCHD2
Normal
Tumor
Relative DNA Amount of EGFR
102
52
3
2
1
0
S3
S4
S5
S10
GBM samples
E
13q14 Del (RB)
Normal
Del
p=0.0224
F
17p13.1 Del/AUPD (p53)
Normal
Del/AUPD
p=0.00603

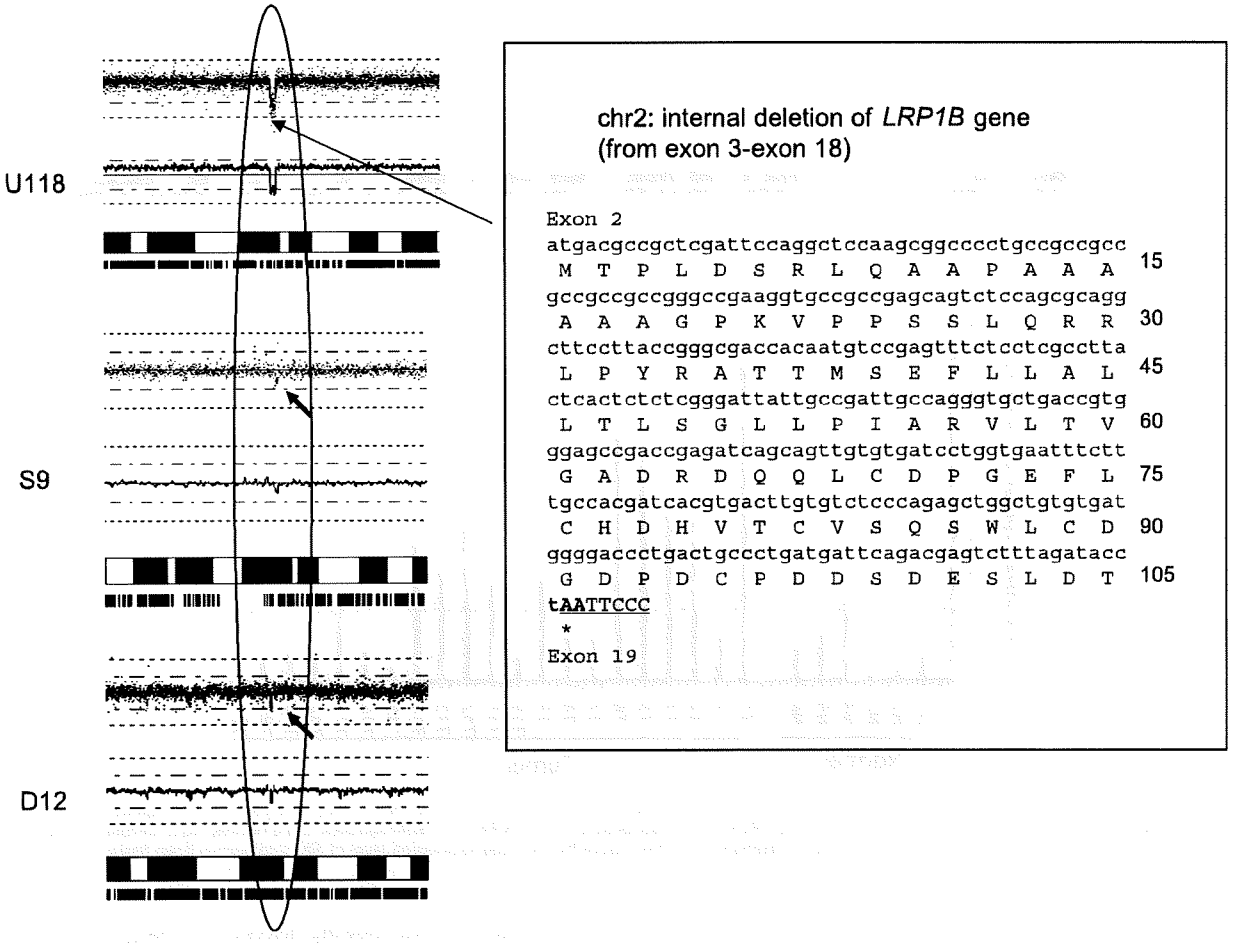

FIGURE 2. Internal deletion of *LRP1B* in GBM. Representative deletions of the *LRP1B* gene are shown in the U118 GBM cell line and two GBM samples. The cDNA of *LRP1B* from U118 was sequenced, showing a deletion between exons 3 and 18. This truncated cDNA has an early stop codon after amino acid 105 (TAA). The sequence that is underlined is at exon 19.

GPR157, H6PD in the second region (Fig. 4). One GBM (case c19) had a homozygous deletion in the intron between exons 3 and 4 of *CAMTA1*.

Another common deleted region occurred in 6q. Loss of 6q was discovered in 16 of 55 samples. Two of these GBMs had a homozygous deletion at 6q26-27, including the *PARK2, PACRG, QKI*, and *PDE10A* genes (Fig. 5A). The expression of *PARK2* in 34 of 56 additional GBM samples (61%) was lower than the 50% mean level present in normal brain tissue (Fig. 5B).

AUPD at 17p in GBM

One of the advantages of the SNP-Chip technique is the ability to identify AUPD. During carcinogenesis, the abnormal allele is often duplicated and the normal matched allele is deleted, resulting in the duplication of the abnormal allele. A total of 32 AUPDs were found in 55 tumor samples and eight of these AUPDs were at the same region of 17p, which included the *p53* gene (Fig. 6A). The 17p AUPDs were validated using several different approaches. As might be predicted, the

FIGURE 1. Representative SNP-Chip analysis and validation of GBM samples. **A.** 9p21.3 deletions: Four representative patterns of chromosome 9p21.3 deletions in GBM samples detected by SNP-Chip. Blue lines above each chromosome show total gene dosage; level 2 indicates diploid (2N) amount of DNA, which is normal. Green bars under each chromosome indicate the SNP sites showing heterozygosity in GBM samples. When heterozygosity is not detected in the tumor but is found in its matched normal control, the result suggests that the GBM has allelic imbalance in that region. The bottom lines in each panel show allele-specific gene dosage (one line indicates gene dosage of the paternal allele and the other indicates the gene dosage of the maternal allele). Level 1 is normal for each gene dosage. Six representative samples with 9p21.3 homozygous deletion with a CMDR containing *CDKN2A* and *CDKN2B* are shown. **B.** Data validation: DNA dose of *CDKN2A* was measured by Q-PCR. Stripe columns, the DNA dose in GBM samples; black columns, DNA dose in their matched normal controls. Each sample showed homozygous *CDKN2A* deletion by SNP-Chip analysis. **C.** Chromosome 7p11.2 amplicon: Four representative GBM samples with amplification at chromosome 7p11.2 are shown. The CMAR contains *EGFR, ECOP, LANCL2, FKBP9L, GBAS, PSPH, CCT6A, SUMF2, PHKG1*, and *CHCHD2* genes. **D.** Data validation: DNA dose of *EGFR* was measured by Q-PCR. Stripe columns, relative DNA amounts in GBM samples; black columns, DNA dose in their matched normal controls. Each sample showed *EGFR* amplification by SNP-Chip analysis. Kaplan-Meier estimates of overall survival for patients with and without 13q14 Del (RB; **E**) and 17p13.1 Del/AUPD (p53; **F**). Tick marks indicate censored data. Prognosis is worse for patients with a deletion of 13q14 ($P = 0.0224$ by the log-rank test) and deletion/AUPD of 17p13.1 ($P = 0.00603$).

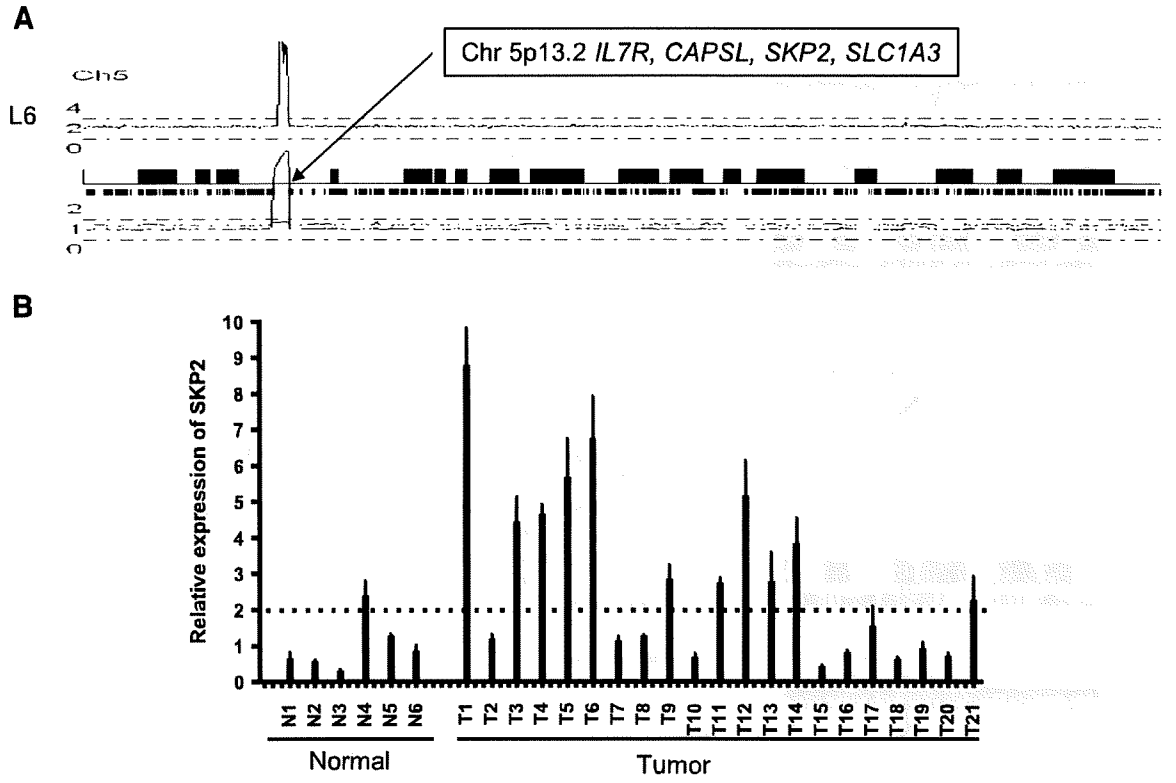

FIGURE 3. Amplicon at chromosome 5p13.2. **A.** Amplification of chromosome 5p13.2 containing the *IL7R, CAPSL, SKP2,* and *SLC1A3* genes is detected in one GBM sample (*L6*). **B.** Real-time reverse transcription-PCR measured expression of *SKP2* in 21 GBM samples and 6 normal brain samples (status of *SKP2* gene copy number in these samples is unknown). Dashed line, 2-fold above the average expression level of *SKP2* in normal brain tissue.

quantity of DNA at this 17p chromosomal region was normal when comparing the samples having AUPD with their matched normal DNAs (Fig. 6B). Moreover, LOH analysis using a microsatellite marker on 17p13.3 showed loss of one of the normal alleles when comparing tumor and matched normal control DNA (Fig. 6C). Homozygous p53 mutations (from exons 5 to 8) were identified by nuclear sequencing the shifted bands identified by single-strand conformational polymorphism (SSCP). Of the eight tumor samples with AUPD, one sample (S1) had a 254I deletion, another (S9) had a R175H mutation (Fig. 6D), and two cases had a R248Q mutation. Also, 17p AUPD encompassing the *p53* gene was found in the U118, U138, U343, U373, and T98G GBM cell lines. Nucleotide sequencing showed that each of these cell lines had a homozygous mutant *p53* with loss of the normal *p53* allele (Fig. 6D and data not shown). In contrast, no chromosome 17p AUPD was found in the U87 GBM cell line, and this cell line had a wild-type *p53* gene (data not shown).

Discussion

High-density SNP-Chip arrays allow rapid detection of amplifications, deletions, and AUPD. This novel technique greatly increases sensitivity of detection of copy number changes in small regions of the genome using only 250 ng genomic DNA. A 250K SNP-Chip interrogates on average about every 12-kb genome, often allowing detection of changes within a gene. Comparative genomic hybridization (CGH) is another technique to examine tumors for an overview of the genome. CGH has been used to detect the chromosome imbalances and molecular classification in gliomas (15-17). Unlike CGH, SNP-Chip technique can detect AUPD. As shown by our study, AUPD is very frequent in GBM. Two previous studies also analyzed genomic abnormalities in gliomas by the SNP-Chip technique (4, 18). One of these was a multi-institutional study that incorporated several genomic approaches, including SNP-Chip, sequencing, and microarray expression analysis (4). Their studies and ours confirmed that this technique is a useful tool to identify novel genomic changes in GBM and a number of common abnormalities were identified including regions of AUPD.

AUPD can be identified by LOH analysis plus quantification of the DNA within the region; however, these abnormalities are more quickly and robustly identified by SNP-Chip analysis. A study of various cancer cell lines found on average 4.7 AUPDs per cell line (19). AUPD results in a duplicated chromosomal region containing either a mutated, inactivated tumor suppressor gene or mutated, activated oncogene. For example, we found frequent AUPD at 17p in GBM samples that contained a mutant p53; thus, the AUPD resulted in duplication of the mutant p53 and loss of the normal p53 allele. GBMs seem to favor duplicating the mutant *p53* (AUPD) rather than

merely deleting the normal allele and keeping one copy of the mutant *p53*. Missense mutation resulting in an expressed protein with a long half-life is the most frequent alteration in cancer (20). The p53 protein forms tetramers. Mutant p53 might either behave in a dominant-negative fashion or have a gain of function and contribute to oncogenic activities *in vitro* and *in vivo* (21). For example, knock-in mice carrying one null allele and one mutant allele of the *p53* gene developed novel tumors compared with p53-null mice (22-26).

A recent SNP-Chip study showed that the *EGFR* located at chromosome 7p11.2 was amplified in up to 43% GBM samples (4), and amplification of the gene was associated with overexpression of the EGFR protein in GBM (9). We found that 19 of 55 GBMs (35%) had trisomy of chromosome 7 or duplication of chromosome 7p, and another 17 of 55 (31%) GBM had prominent amplification of the *EGFR* gene. The SNP-Chip analysis showed that at least nine additional genes were coamplified with *EGFR*. Of note, some breast cancers with amplification of *Her2/neu* (*EGFR-2*) also contain the *topoisomerase 2* (*TOPO-2*) gene in the same amplicon. These patients have an increased response when treated with both an inhibitor of TOPO-2 and trastuzumab (Herceptin, a monoclonal antibody that targets Her-2/neu; ref. 27). Further studies of the genes in the *EGFR* amplicon may offer additional therapeutic targets for GBM. Also, *VEGFR* and *PDGFRA* were in an amplicon or involved in trisomy on chromosome 4q11-12 in 5 of 55 (9%) GBM samples. In a recent study, high-level amplification of *VEGFR/PDGFRA* occurred in 13% samples (4). Amplification and presumably abundant expression of these genes may allow for autocrine and paracrine stimulation of growth. These tumors may be more sensitive to inhibitors of these receptors or their growth factors [e.g., bevacizumab (Avastin)].

We found that the *SKP2* gene on chromosome 5p was markedly amplified in a GBM sample and its expression was increased >2-fold compared with normal brain tissue in 11 of 21 additional GBM samples. SKP2 is required for ubiquitin-mediated degradation of the CDK inhibitor p27 (28). Saigusa et al. reported amplification of DNA at chromosome 5p in the region of *SKP2* in four glioma cell lines and also found that the expression of the *SKP2* gene was increased in 31% of primary GBM examined by immunohistochemistry (29). They found that increased expression of SKP2 was associated with an

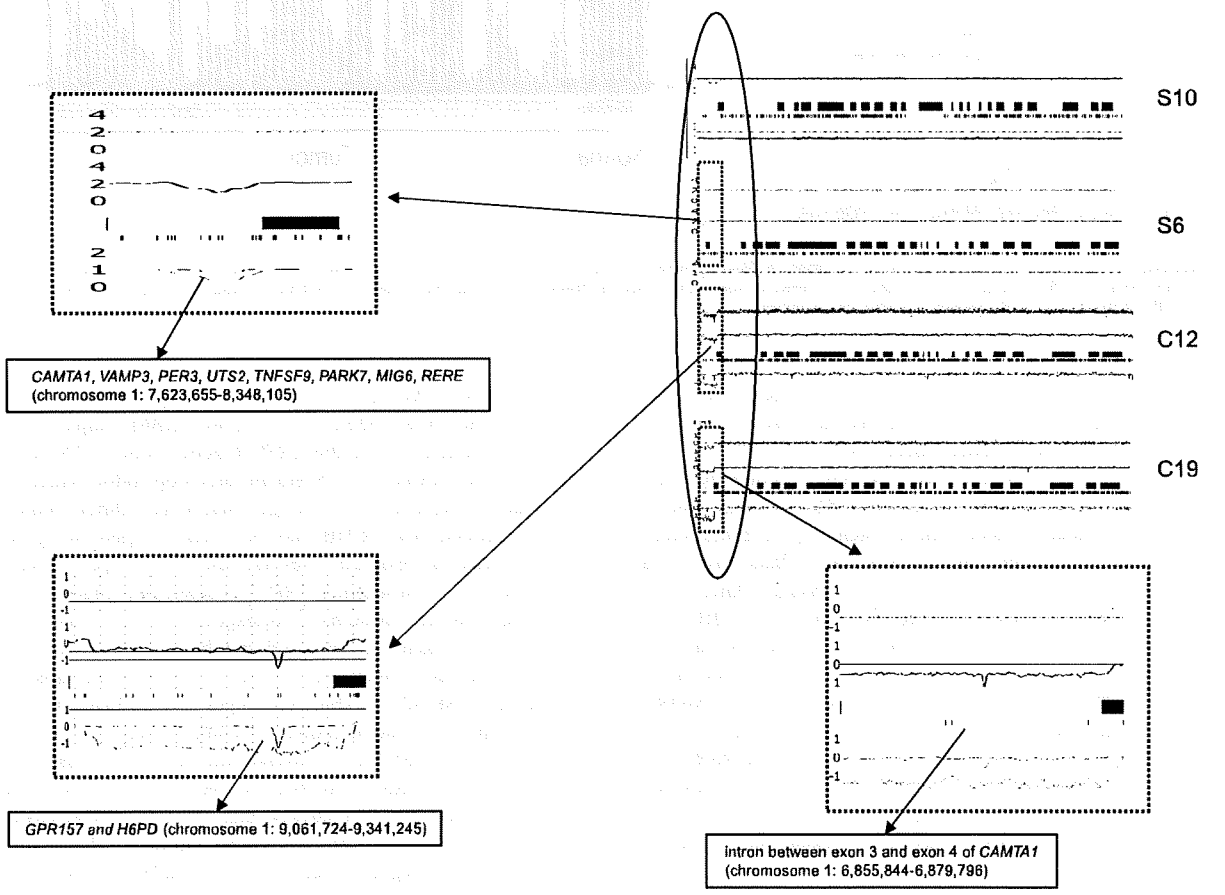

FIGURE 4. Chromosome 1p36 deletion in GBM. Four representative deletions as detected by SNP-Chip at 1p36 (*top right*). Heterozygous (S10) and homozygous (S6, C12, C19) deletions occur at two CMDRs containing the *CAMTA1, PER3, UTS2, TNFSF9, VAMP3, PARK7, MIG6,* and *RERE* genes (*top left*), *GPR157* and *H6PD* genes (*bottom left*). A homozygous deletion within the intron between exons 3 and 4 of *CAMTA1* occurred in the GBM sample C19 (*bottom right*).

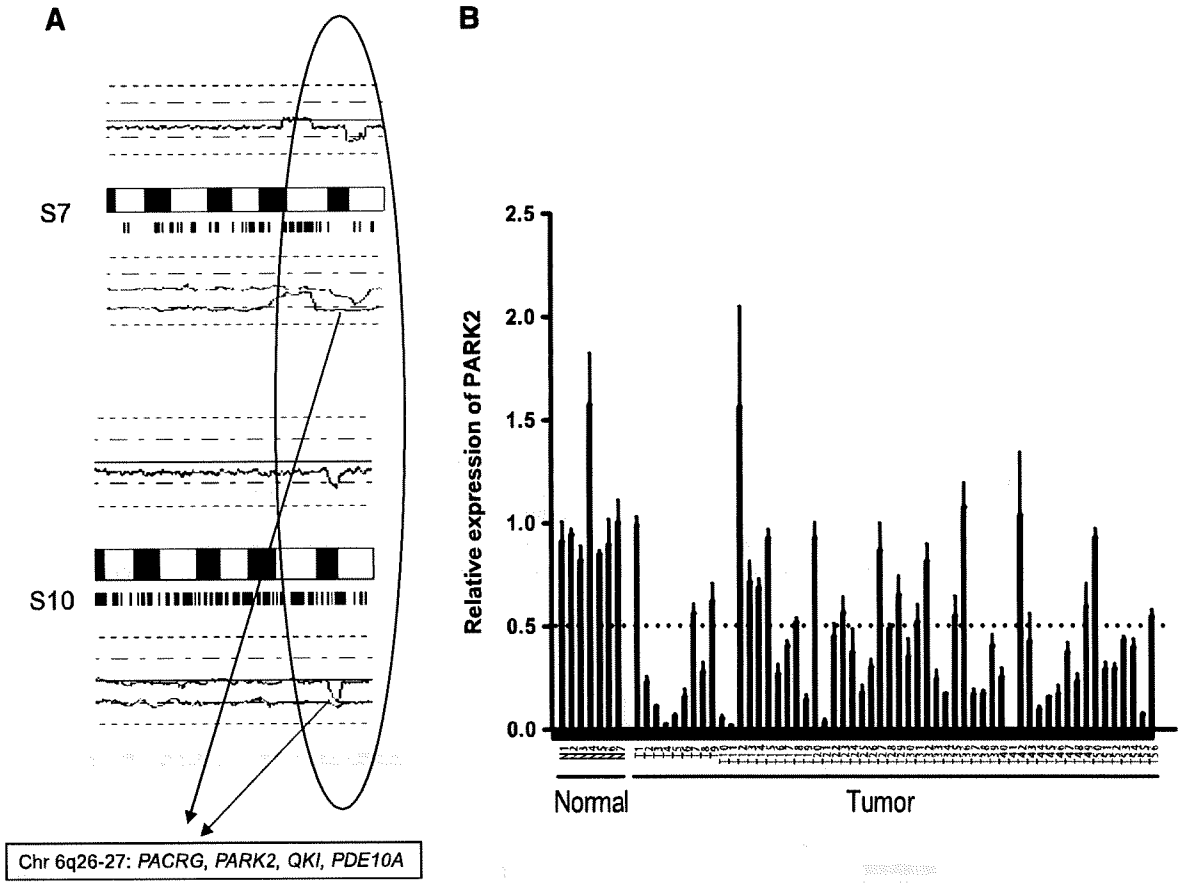

FIGURE 5. Chromosome 6q26-27 deletion in GBM. **A.** Representative samples with chromosome 6q26-27 deletions. CMDR contains *PACRG, PARK2, QKI,* and *PDE10A*. **B.** Expression of *PARK2* in 56 GBM samples and 7 normal brain samples as measured by real-time reverse transcription-PCR. Dotted line, 50% of the mean level present in normal brain tissue.

overall shorter survival (29). High levels of SKP2 have also been associated with cancers of the thyroid (30) and the lung (31, 32), as well as neuroblastomas (33).

The short arm of chromosome 1 at 1p36 is frequently deleted in hematopoietic malignancies (34, 35), epithelial cancers (36, 37), and neural-related cancers, including neuroblastomas (38), meningiomas (39), and gliomas (40). Allelic loss at 1p has been reported in 20% to 30% of astrocytomas. Other investigators defined a 150-kb CMDR on 1p36.23 by LOH mapping, which encompassed *CAMTA1*, a gene encoding a transcription factor (41). We also discovered 1p deletions in 19 of 55 GBM samples (35%), which included two CMDRs. One contained the *CAMTA* gene alone or the *CAMTA* gene plus *PER3, UTS2, TNFSF9, VAMP3, PARK7, MIG6,* and *RERE*; the second CMDR had both of the *GPR157* and *H6PD* genes in a sample. Further studies are required to determine if *CMTA* is the key target gene of 1p36 deletion in various cancers including GBM.

The *LRP1B* gene is highly homologous to the lipoprotein receptor-related protein 1 (LRP1, a family member of the low-density lipoprotein receptors). *LRP1B* has been classified as a tumor suppressor gene and is frequently mutated in GBM (42-47). We discovered a novel internal deletion of *LRP1B* in the U118 GBM cell line and four GBM samples. Nucleotide sequencing of the *LRP1B* gene from U118 cells showed loss of exons 3 to 18 and an early stop codon, suggesting that the protein was no longer functional. Other studies have suggested that LRP1B may be a tumor suppressor gene that is deleted or abnormal in several other tumor types, as well as GBM (42-47). In addition, *LRP1B* is deleted or epigenetically silenced in oral urothelial, esophageal, and non–small-cell lung cancers; taken together, *LRP1B* behaves as a tumor suppressor gene that is frequently mutated in several solid tumors, including GBM (42-47). Our data suggest that *LRP1B* acts as a tumor suppressor gene in glioma cells and is aberrant in GBM.

Deletion of ~165 Mb of chromosome 6q25-27 in GBM involving *IGF2R, PARK2, PACRG,* and *QKI* was found by CGH (40). Our SNP-Chip data showed that 16 of 55 (29%) GBM samples had deletion of chromosome 6q and two of these samples had a homozygous deletion (4%) at 6q26-27, which included the *PARK2, PACRG, QKI,* and *PDE10A* genes. In another large study, 54 deletions of this region were found in a total of 206 (26%) GBM samples, including six homozygous deletions (3%; ref. 4). The *PARK2* gene has been reported to be

mutated in some patients with autosomal recessive juvenile Parkinson's disease, and investigators recently suggested that the gene is a candidate tumor suppressor gene in ovarian and breast cancers as well as leukemias (48-50). *PARK2* shares a bidirectional promoter with *PACRG*. Abnormal methylation of this common promoter was observed in 26% of acute lymphoblastic leukemia and 20% of chronic myelogenous leukemia in lymphoid blast crisis and was associated with decreased expression of both of these genes (48). We found that ~61% (34 of 56) of GBM samples had 50% decreased expression of *PARK2* compared with normal control brain tissues. Our data suggest that *PARK2* behaves as a tumor suppressor gene that is inactivated in GBM.

In a large comprehensive study, deletion at chromosome 10q23.3 (contains *PTEN* gene) was found in ~173 of 206 (84%) GBMs, including homozygous deletions of the *PTEN* gene in 9 of 206 (4%) samples (4). Further studies found that *PTEN* was mutated in 44% of GBM, and 60% of those with LOH at 10q had a mutant *PTEN* gene (51). PTEN is an inhibitor of the phosphoinositide 3-kinase mammalian target of rapamycin/AKT pathway that is downstream of EGFR or VEGFR/PDGFRA in this growth stimulatory pathway. In our study, 33 of 55 (60%) GBM samples had lost a *PTEN* allele. Two samples (4%) had homozygous deletion of this gene. Taken together, 71% of GBM samples had either deletion of *PTEN* or amplification/trisomy of *EGFR* and/or *VEGFR/PDGFRA*.

The cyclin-dependent kinase inhibitor p16(INK4A) normally inhibits CDK4 and CDK6, resulting in dephosphorylation of Rb. This ensures that Rb continues to bind and inactivate E2F (cell cycle transcription factor), maintaining a brake on the cell cycle. The p16(INK4A)-CDK4/6-Rb pathway is aberrant in the vast majority of GBMs (1, 2). The *p16(INK4A)*, *p15(INK4B)*, and *p14(ARF)* (inhibitor of MDM2) genes are contiguous on chromosome 9. We found that all three genes were lost in 35 of 55 (64%) GBM samples, either by homozygous or hemizygous deletion. Also, 30 of 55 GBMs had trisomy of chromosome 7, resulting in three copies of *CDK6*; 6 of 55 GBM samples had amplification of *CDK4* on chromosome 12. In addition, the *Rb* gene (chromosome 13q14.2-14.3) was deleted in 22 of 55 GBM samples. Taken together, the p16(INK4A)/p15 (INK4B)-CDK4/6-pRb pathway was structurally aberrant in 48 of 55 GBM (87%) samples.

The p14(ARF) binds to MDM2 and MDM4, preventing them from decreasing the level of p53. Loss of *p14(ARF)* or amplification of *MDM2/MDM4* lead to inactivation of p53. We found that either the *MDM4* (1q32.1) or the *MDM2* (12q15) gene was increased in copy number in 13 of 55 (24%) GBMs, *p14(ARF)* was deleted in 35 of 55 (64%) cases, and 18 of 55 (33%) samples had either AUPD or deletion of p53. Thus, the p14(ARF)-MDM2/4-p53 pathway was structurally aberrant in 48 of 55 GBM (87%) samples. Ghimenti et al. noted alterations of the p14(ARF)-MDM2-p53 pathway in 73%

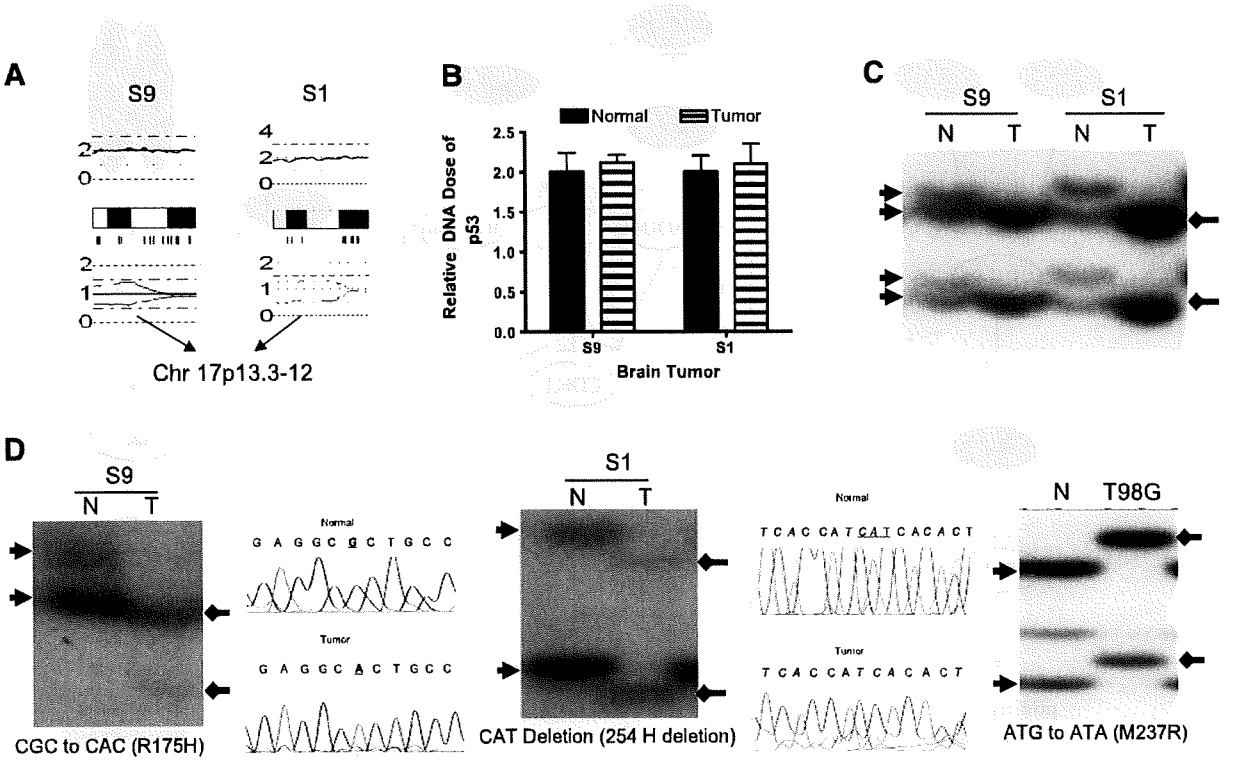

FIGURE 6. Chromosome 17p13.3-12 AUPD in GBM. **A.** Two representatives examples of AUPD at chromosome 17p13.3-12. **B.** DNA level of p53 was measured by real-time quantitative PCR. Striped and black bars, DNA amount in GBM samples and their matched normal control, respectively. **C.** Microsatellite marker (chr17:1857382-1857419) was used to analyze LOH in tumor samples compared with their normal matched controls (→, band pattern in normal samples; →, band pattern in tumor samples). **D.** DNA of three GBM samples was analyzed for p53 mutations initially by SSCP (→, band pattern in normal samples; →, band pattern in tumor samples). Nucleotide sequencing: G changed to A in S9; deletion of CAT in S1; and G changed to A (M237R) in T98G (sequence data not shown).

of GBM samples (52). We found that the frequency of amplification/trisomy of *MDM4* was similar to amplification of *MDM2* in GBM samples and both rarely coexisted in the same sample. This is consistent with previous reports (53, 54). Taken together, abnormalities of the EGFR/VEGFR/PDGFRA-PTEN (71%), p16(INK4A)/p15(INK4B)-CDK4/6-pRb (87%), and p14(ARF)-MDM2/4-p53 (87%) pathways were present in the vast majority of GBM samples, and almost all GBM (91%) samples had an abnormality of at least one of the three pathways (Fig. 7). Congruent with our study, alteration in these three core pathways was noted in 78% to 88% of GBM samples in a large cooperative study (4). The proteins of these pathways provide therapeutic targets for GBM. These include EGFR inhibitors, such as erlotinib and gefitinib (55), dual inhibitors of PI3K and mTOR, including the investigational drug PI-103 (56) and inhibitors of mTOR [e.g., rapamycin (57) and Everolimus (58)].

The aberrant genes in GBM are incompletely identified. Present-day clinical and therapeutic management often relies on 50- to 100-year-old techniques of morphology and immunochemistry. SNP-Chip is an extremely robust technology, offering the opportunity to discover, in a potentially simple fashion, copy number changes, including AUPD associated with GBM. The patterns of genetic abnormalities, even in the absence of knowledge of the specific genetic lesions, may result in a useful, new GBM classification. Furthermore, new genetic lesions identified by SNP chip may become targets for novel therapies.

Materials and Methods

Clinical Samples, Cell Cultures, and DNA Preparation

GBM from 55 individuals were studied by SNP-Chip. The age of these patients ranged from 18 to 70 years. Twenty-two of these 55 samples had matched peripheral blood neutrophils from the same patients. Also, 4 of the 55 GBM samples were established explants as previously described (59) and used for SNP analysis. Furthermore, six human GBM cell lines (U87, U118, U138, U343, U373, and T98G) were used for SNP-Chip studies. Standard proteinase K-phenol-chloroform extraction method was used to extract DNA from GBM samples, cell lines, and explants. In addition, 56 additional GBM samples were quick frozen, and RNA was extracted and used for expression analysis of target genes. Written informed consent for research use of all of these samples was obtained before surgery, according to a protocol approved by the institutional ethics committee. Cell lines were maintained in DMEM (Life

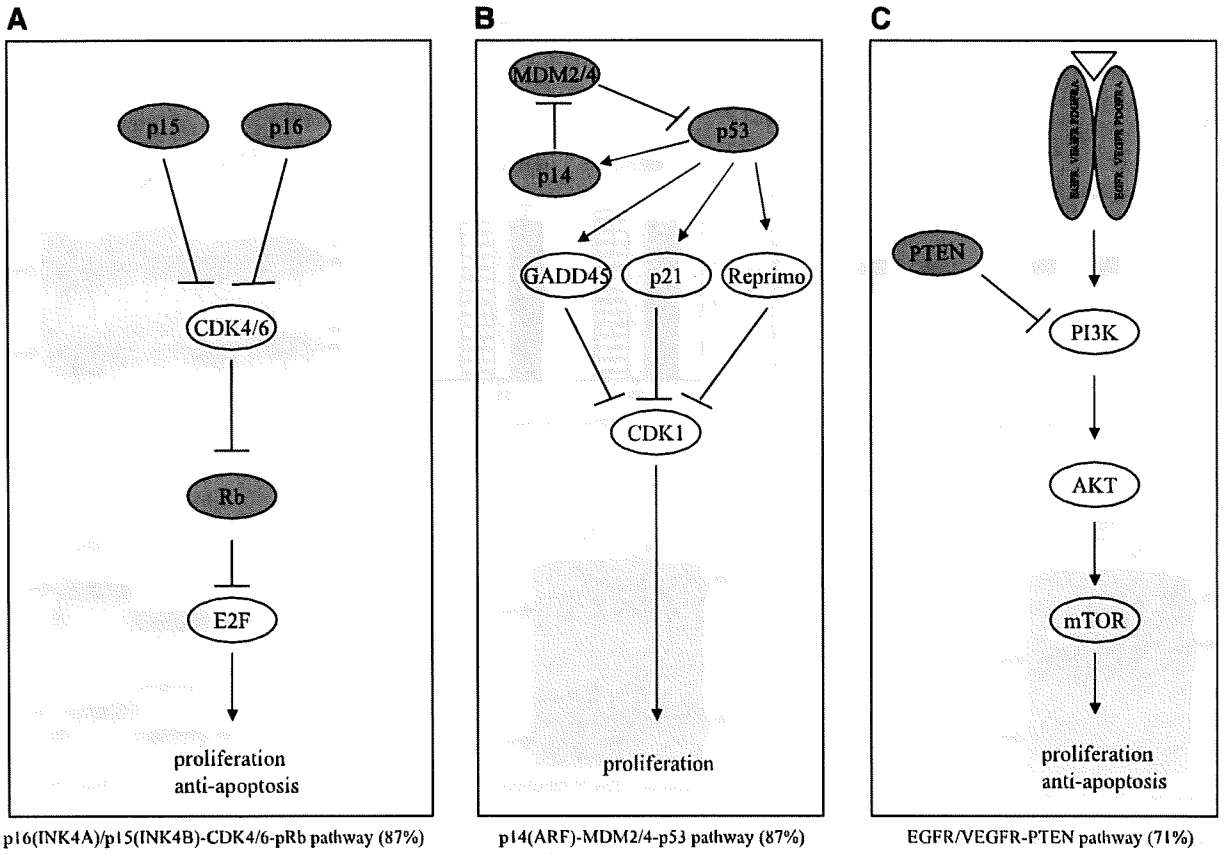

FIGURE 7. Major functional pathways dysregulated in GBM as detected by SNP-Chip. **A.** Cell cycle pathway (G_1-S): p16(INK4A)/p15(INK4B)-CDK4/6-pRb (genomic abnormality in 87% of samples). **B.** p53 pathway: p14(ARF)-MDM2/4-p53 (genomic abnormality in 87% of samples). **C.** Growth factor receptor (EGFR/VEGFR/PDGFA) and secondary signaling pathway (genomic abnormality in 71% of samples). Gray circles, aberrant genes analyzed by SNP-Chip. %, percentage of GBM samples with abnormality in the pathway.

Table 3. Oligonucleotide Primer Sequences Used for Real-time Q-PCR for DNA and cDNA

Gene	Oligonucleotide	Sequence	Melting temperature (°C)
CH2p21-DNA internal control	Forward	5′-GGCAATCCTGGCTGCGGATCAAGA	81
	Reverse	5′-ATTTCTGAACTTCTTGGCTGCC	
p16-DNA	Forward	5′-GTGCCAAAGTGCTCCTGAAGCTG	80
	Reverse	5′-AGCAAATCTGTTTGGAGGTCTG	
PARK2-cDNA	Forward	5′-CGTGCACAGACGTCAGGAG	85
	Reverse	5′-AAGGCAGGGAGTAGCCAAGT	
SKP2-cDNA	Forward	5′-TGGTATCGCCTAGCGTCTG	85
	Reverse	5′-ACACGAAAAGGGCTGAAATG	
EGFR-DNA	Forward	5′-CAGGAGGTGGCTGGTTATGT	82
	Reverse	5′-ATGGGCAGCTCCTTCAGTC	
p53-DNA	Forward	5′-CTTGGGCCTGTGTTATCTCC	84
	Reverse	5′-TCTTCCAGTGTGATGATGGTGG	
β-actin-cDNA	Forward	5′-TCCCTGGAGAAGAGCTACGA	87
	Reverse	5′-GGAAGGAAGGCTGGAAGAG	

Technologies) with 10% FCS (Gemini Bio-Products), 10 units/mL penicillin G, and 10 mg/mL streptomycin (Gemini Bio-Products). All cells were incubated at 37°C in 5% CO_2.

High-Density SNP-Chip Analysis

SNP-Chips for human 50K *Xba*I/250K Nsp arrays were used for this study (SNP-Chip, Affymetrix). The DNA samples from 22 GBM patients with matched peripheral blood neutrophils from the same patient as control DNA were analyzed by 50K SNP-Chips as previously described (60). The other 33 DNA samples without matched control DNA and six human GBM cell lines were analyzed by 250K SNP-Chips, using allele-specific copy number analysis using anonymous references (AsCNAR; ref. 61). Fragmentation and labeling of DNAs were done using a GeneChip resequencing kit (Affymetrix); hybridization, washing, and signal detection were done on a GeneChip Fluidics Station 400 and GeneChip scanner 3000 according to the manufacturer's protocols (Affymetrix). Microarray SNP data were analyzed for determination of both total and allelic-specific copy number using the CNAG program with AsCNAR capability,[7] as we have previously described (47, 48). In the latter algorithm, AsCNs were estimated using "nonpaired" genomic DNA as controls, where array signals at the heterozygous SNP sites in the tumor sample are compared with the corresponding signals in one or more control samples also showing the heterozygous SNP calls. All the SNPs within an inferred LOH region are formally analyzed as heterozygous SNPs (see ref. 48 for mathematical details). Control sample sets used for allelic-specific copy number calculations may be different from SNP to SNP. AsCNAR enables detection of LOH regions in those samples highly contaminated with normal cells and provides an accurate measurement of total copy numbers (48). Size, position, and location of genes were identified with the University of California, Santa Cruz Genome Browser.[8] Our software allows accurate calls of AUPD and copy number changes without requiring germline DNA. All known copy number polymorphism were eliminated from analysis by using the UCSC Genome Browser. All the raw data of these SNP-Chips have been submitted to the public database ArrayExpress.[9] The ArrayExpress accession number is E-MEXP-1330.

Quantitative-PCR

Total RNA was extracted using TRIzol (Invitrogen) according to the manufacturer's protocol. DNA was removed by DNase. Two micrograms of RNA were reverse transcribed with random primers and Superscript III reverse transcriptase (Invitrogen). The cDNA was used for real-time PCR with Platinum Taq (Invitrogen) and SYBRGreen I (Molecular Probes) in triplicates in an iCycler iQ system (Bio-Rad). The PCR conditions were as follows: 2 min at 94°C followed by 45 cycles of 94°C for 15 s, 60°C for 15 s, 72°C for 15 s, and fluorescence determination at the melting temperature of the product for 20 s. Specificity of PCR products was checked on agarose gel. The expression of β-actin was used as an endogenous reference. A comparative threshold cycle was used to determine target genes and β-actin gene expression relative to the no-sample control (calibrator). The mRNA expression level was normalized by β-actin expression. The relative expression level of target genes in control samples was normalized to a relative value of 1. Final results in treated samples were expressed as *n*-fold difference to the control samples. The DNA dose also was measured by real-time quantity PCR as described above. The sequences of primers are shown in Table 3.

SSCP and Nucleotide Sequencing

For detection of *p53* mutations using SSCP, each PCR reaction contained 20 ng DNA, 10 pmol of each of the primers, 2 nmol/L of each of deoxynucleotide triphosphate, 0.5 units of Taq DNA polymerase, and 3 μCi [α-^{32}P]dCTP in 20 μL. PCR products were diluted 10-fold in the loading buffer containing 10 mmol/L NaOH, 95% formamide, and 0.05% of both bromophenol blue and xylene cyanol. After denaturation at 94°C for 5 min, 2 μL of the samples were loaded onto a 6% nondenaturation polyacrylamide mutation detection enhancement gel (MDE Bioproducts) with 10% (v/v) glycerol and electrophoresed at 4 to 6 W for 20 h. Subsequently, the gel was dried and subjected to autoradiography. Single-strand DNAs of mutant candidate

[7] http://www.genome.umin.jp/
[8] http://genome.ucsc.edu/
[9] http://www.ebi.ac.uk/microarray-as/ae/

bands showed aberrant migration through SSCP analysis. These shifted bands were excised and eluted by diffusion in 50 μL TE buffer. One microliter of elution TE was used as template to reamplified the fragment. The resulting product was sequenced using the Big-dye sequence reaction (Applied Biosystems) and analyzed on an Autosequencer 3100. The *p53* gene was analyzed for mutations in exons 5 to 8 (62).

LOH Analysis

PCR amplification of microsatellite sequences was used to determine LOH on chromosome 17p. Primers for amplification of the microsatellite fragments (chr17:1857382-1857419) were 5′-CGCCTTTCCTCATACTCCAG and 5′-GCCAGACGGGACTTGAATTA. Each PCR reaction contained 25 ng of DNA, 10 pmol of each primer, 2 nmol of each deoxynucleotide triphosphate, 0.5 units of *Taq* DNA polymerase, and 3 μCi of [α-^{32}P] dCTP in 20 μL of the specified buffer with 1.5 mmol/L $MgCl_2$. Thirty-two cycles of amplification, PAGE, and subsequent autoradiography were done as published previously (63).

Statistical Analysis

Overall survival was analyzed with the Kaplan-Meier method to assess prognostic significance of the observed genomic abnormalities. We applied the log-rank test to compare patients with and without a specific genomic abnormality. *P* values were not adjusted for multiple testing. Analyses were done in R[10] using survival package version 2.34-1.

Disclosure of Potential Conflicts of Interest

No potential conflicts of interest were disclosed.

[10] http://www.R-project.org

References

1. Schmidt EE, Ichimura K, Reifenberger G, Collins VP. CDKN2 (p16/MTS1) gene deletion or CDK4 amplification occurs in the majority of glioblastomas. Cancer Res 1994;54:6321–4.

2. Ueki K, Ono Y, Henson JW, Efird JT, von Deimling A, Louis DN. CDKN2/p16 or RB alterations occur in the majority of glioblastomas and are inversely correlated. Cancer Res 1996;56:150–3.

3. Ohgaki H, Dessen P, Jourde B, et al. Genetic pathways to glioblastoma: a population-based study. Cancer Res 2004;64:6892–9.

4. McLendon R, Friedman A, Bigner D, et al. Comprehensive genomic characterization defines human glioblastoma genes and core pathways. Nature 2008;1061–8.

5. Merlo A, Herman JG, Mao L, et al. 5′ CpG island methylation is associated with transcriptional silencing of the tumour suppressor p16/CDKN2/MTS1 in human cancers. Nat Med 1995;1:686–92.

6. Nishikawa R, Furnari FB, Lin H, et al. Loss of P16INK4 expression is frequent in high grade gliomas. Cancer Res 1995;55:1941–5.

7. Arap W, Nishikawa R, Furnari FB, Cavenee WK, Huang HJ. Replacement of the p16/CDKN2 gene suppresses human glioma cell growth. Cancer Res 1995;55:1351–4.

8. Henson JW, Schnitker BL, Correa KM, et al. The retinoblastoma gene is involved in malignant progression of astrocytomas. Ann Neurol 1994;36:714–21.

9. von Deimling A, Louis DN, von Ammon K, et al. Association of epidermal growth factor receptor gene amplification with loss of chromosome 10 in human glioblastoma multiforme. J Neurosurg 1992;77:295–301.

10. Duerr EM, Rollbrocker B, Hayashi Y, et al. PTEN mutations in gliomas and glioneuronal tumors. Oncogene 1998;16:2259–64.

11. Li J, Yen C, Liaw D, et al. PTEN, a putative protein tyrosine phosphatase gene mutated in human brain, breast, and prostate cancer. Science 1997;275:1943–7.

12. Steck PA, Pershouse MA, Jasser SA, et al. Identification of a candidate tumour suppressor gene, MMAC1, at chromosome 10q23.3 that is mutated in multiple advanced cancers. Nat Genet 1997;15:356–62.

13. Narita Y, Nagane M, Mishima K, Huang HJ, Furnari FB, Cavenee WK. Mutant epidermal growth factor receptor signaling down-regulates p27 through activation of the phosphatidylinositol 3-kinase/Akt pathway in glioblastomas. Cancer Res 2002;62:6764–9.

14. Hayashi Y, Ueki K, Waha A, Wiestler OD, Louis DN, von Deimling A. Association of EGFR gene amplification and CDKN2 (p16/MTS1) gene deletion in glioblastoma multiforme. Brain Pathol 1997;7:871–5.

15. Roerig P, Nessling M, Radlwimmer B, et al. Molecular classification of human gliomas using matrix-based comparative genomic hybridization. Int J Cancer 2005;117:95–103.

16. Bourdon V, Plessis G, Chapon F, Guarnieri J, Derlon JM, Jonveaux P. Chromosome imbalances in oligodendroglial tumors detected by comparative genomic hybridization. Ann Genet 2004;47:105–11.

17. Paunu N, Sallinen SL, Karhu R, et al. Chromosome imbalances in familial gliomas detected by comparative genomic hybridization. Genes Chromosomes Cancer 2000;29:339–46.

18. Kotliarov Y, Steed ME, Christopher N, et al. High-resolution global genomic survey of 178 gliomas reveals novel regions of copy number alteration and allelic imbalances. Cancer Res 2006;66:9428–36.

19. Zhao X, Li C, Paez JG, et al. An integrated view of copy number and allelic alterations in the cancer genome using single nucleotide polymorphism arrays. Cancer Res 2004;64:3060–71.

20. Blagosklonny MV. p53 from complexity to simplicity: mutant p53 stabilization, gain-of-function, and dominant-negative effect. FASEB J 2000;14:1901–7.

21. Kim E, Deppert W. Transcriptional activities of mutant p53: when mutations are more than a loss. J Cell Biochem 2004;93:878–86.

22. Lang GA, Iwakuma T, Suh YA, et al. Gain of function of a p53 hot spot mutation in a mouse model of Li-Fraumeni syndrome. Cell 2004;119:861–72.

23. Bossi G, Lapi E, Strano S, Rinaldo C, Blandino G, Sacchi A. Mutant p53 gain of function: reduction of tumor malignancy of human cancer cell lines through abrogation of mutant p53 expression. Oncogene 2006;25:304–9.

24. Olive KP, Tuveson DA, Ruhe ZC, et al. Mutant p53 gain of function in two mouse models of Li-Fraumeni syndrome. Cell 2004;119:847–60.

25. Heinlein C, Krepulat F, Lohler J, Speidel D, Deppert W, Tolstonog GV. Mutant p53(R270H) gain of function phenotype in a mouse model for oncogene-induced mammary carcinogenesis. Int J Cancer 2008;122:1701–9.

26. Scian MJ, Stagliano KE, Anderson MA, et al. Tumor-derived p53 mutants induce NF-κB2 gene expression. Mol Cell Biol 2005;25:10097–110.

27. Jarvinen TA, Liu ET. Simultaneous amplification of HER-2 (ERBB2) and topoisomerase IIα (TOP2A) genes—molecular basis for combination chemotherapy in cancer. Curr Cancer Drug Targets 2006;6:579–602.

28. Carrano AC, Eytan E, Hershko A, Pagano M. SKP2 is required for ubiquitin-mediated degradation of the CDK inhibitor p27. Nat Cell Biol 1999;1:193–9.

29. Saigusa K, Hashimoto N, Tsuda H, et al. Overexpressed Skp2 within 5p amplification detected by array-based comparative genomic hybridization is associated with poor prognosis of glioblastomas. Cancer Sci 2005;96:676–83.

30. Chiappetta G, De Marco C, Quintiero A, et al. Overexpression of the S-phase kinase-associated protein 2 in thyroid cancer. Endocr Relat Cancer 2007;14:405–20.

31. Zhu CQ, Blackhall FH, Pintilie M, et al. Skp2 gene copy number aberrations are common in non-small cell lung carcinoma, and its overexpression in tumors with ras mutation is a poor prognostic marker. Clin Cancer Res 2004;10:1984–91.

32. Salon C, Merdzhanova G, Brambilla C, Brambilla E, Gazzeri S, Eymin B. E2F-1, Skp2 and cyclin E oncoproteins are upregulated and directly correlated in high-grade neuroendocrine lung tumors. Oncogene 2007;26:6927–36.

33. Westermann F, Henrich KO, Wei JS, et al. High Skp2 expression characterizes high-risk neuroblastomas independent of MYCN status. Clin Cancer Res 2007;13:4695–703.

34. Mori N, Morosetti R, Mizoguchi H, Koeffler HP. Progression of myelodysplastic syndrome: allelic loss on chromosomal arm 1p. Br J Haematol 2003;122:226–30.

35. Mori N, Morosetti R, Spira S, et al. Chromosome band 1p36 contains a putative tumor suppressor gene important in the evolution of chronic myelocytic leukemia. Blood 1998;92:3405–9.

36. Kleer CG, Bryant BR, Giordano TJ, Sobel M, Merino MJ. Genetic changes

in chromosomes 1p and 17p in thyroid cancer progression. Endocr Pathol 2000; 11:137–43.

37. Cheung TH, Lo KW, Yim SF, et al. Clinicopathologic significance of loss of heterozygosity on chromosome 1 in cervical cancer. Gynecol Oncol 2005;96: 510–5.

38. White PS, Thompson PM, Gotoh T, et al. Definition and characterization of a region of 1p36.3 consistently deleted in neuroblastoma. Oncogene 2005;24: 2684–94.

39. Piaskowski S, Rieske P, Szybka M, et al. GADD45A and EPB41 as tumor suppressor genes in meningioma pathogenesis. Cancer Genet Cytogenet 2005: 162:63–7.

40. Mulholland PJ, Fiegler H, Mazzanti C, et al. Genomic profiling identifies discrete deletions associated with translocations in glioblastoma multiforme. Cell Cycle 2006;5:783–91.

41. Barbashina V, Salazar P, Holland EC, Rosenblum MK, Ladanyi M. Allelic losses at 1p36 and 19q13 in gliomas: correlation with histologic classification, definition of a 150-kb minimal deleted region on 1p36, and evaluation of CAMTA1 as a candidate tumor suppressor gene. Clin Cancer Res 2005;11: 1119–28.

42. Cengiz B, Gunduz M, Nagatsuka H, et al. Fine deletion mapping of chromosome 2q21-37 shows three preferentially deleted regions in oral cancer. Oral Oncol 2007;43:241–7.

43. Langbein S, Szakacs O, Wilhelm M, et al. Alteration of the LRP1B gene region is associated with high grade of urothelial cancer. Lab Invest 2002;82: 639–43.

44. Liu CX, Musco S, Lisitsina NM, Yaklichkin SY, Lisitsyn NA. Genomic organization of a new candidate tumor suppressor gene, LRP1B. Genomics 2000; 69:271–4.

45. Nakagawa T, Pimkhaokham A, Suzuki E, Omura K, Inazawa J, Imoto I. Genetic or epigenetic silencing of low density lipoprotein receptor-related protein 1B expression in oral squamous cell carcinoma. Cancer Sci 2006;97:1070–4.

46. Roversi G, Pfundt R, Moroni RF, et al. Identification of novel genomic markers related to progression to glioblastoma through genomic profiling of 25 primary glioma cell lines. Oncogene 2006;25:1571–83.

47. Sonoda I, Imoto I, Inoue J, et al. Frequent silencing of low density lipoprotein receptor-related protein 1B (LRP1B) expression by genetic and epigenetic mechanisms in esophageal squamous cell carcinoma. Cancer Res 2004;64: 3741–7.

48. Agirre X, Roman-Gomez J, Vazquez I, et al. Abnormal methylation of the common PARK2 and PACRG promoter is associated with downregulation of gene expression in acute lymphoblastic leukemia and chronic myeloid leukemia. Int J Cancer 2006;118:1945–53.

49. Denison SR, Callahan G, Becker NA, Phillips LA, Smith DI. Characterization of FRA6E and its potential role in autosomal recessive juvenile parkinsonism and ovarian cancer. Genes Chromosomes Cancer 2003;38:40–52.

50. Letessier A, Garrido-Urbani S, Ginestier C, et al. Correlated break at PARK2/FRA6E and loss of AF-6/Afadin protein expression are associated with poor outcome in breast cancer. Oncogene 2007;26:298–307.

51. Wang SI, Puc J, Li J, et al. Somatic mutations of PTEN in glioblastoma multiforme. Cancer Res 1997;57:4183–6.

52. Ghimenti C, Fiano V, Chiado-Piat L, Chio A, Cavalla P, Schiffer D. Deregulation of the p14ARF/Mdm2/p53 pathway and G1/S transition in two glioblastoma sets. J Neurooncol 2003;61:95–102.

53. Riemenschneider MJ, Knobbe CB, Reifenberger G. Refined mapping of 1q32 amplicons in malignant gliomas confirms MDM4 as the main amplification target. Int J Cancer 2003;104:752–7.

54. Riemenschneider MJ, Buschges R, Wolter M, et al. Amplification and overexpression of the MDM4 (MDMX) gene from 1q32 in a subset of malignant gliomas without TP53 mutation or MDM2 amplification. Cancer Res 1999;59: 6091–6.

55. Mellinghoff IK, Wang MY, Vivanco I, et al. Molecular determinants of the response of glioblastomas to EGFR kinase inhibitors. N Engl J Med 2005;353: 2012–24.

56. Fan QW, Cheng CK, Nicolaides TP, et al. A dual phosphoinositide-3-kinase α/mTOR inhibitor cooperates with blockade of epidermal growth factor receptor in PTEN-mutant glioma. Cancer Res 2007;67:7960–5.

57. Cloughesy TF, Yoshimoto K, Nghiemphu P, et al. Antitumor activity of rapamycin in a phase I trial for patients with recurrent PTEN-deficient glioblastoma. PLoS Med 2008;5:e8.

58. Yang L, Clarke MJ, Carlson BL, et al. PTEN loss does not predict for response to RAD001 (Everolimus) in a glioblastoma orthotopic xenograft test panel. Clin Cancer Res 2008;14:3993–4001.

59. Yin D, Zhou H, Kumagai T, et al. Proteasome inhibitor PS-341 causes cell growth arrest and apoptosis in human glioblastoma multiforme (GBM). Oncogene 2005;24:344–54.

60. Nannya Y, Sanada M, Nakazaki K, et al. A robust algorithm for copy number detection using high-density oligonucleotide single nucleotide polymorphism genotyping arrays. Cancer Res 2005;65:6071–9.

61. Yamamoto G, Nannya Y, Kato M, et al. Highly sensitive method for genome-wide detection of allelic composition in nonpaired, primary tumor specimens by use of Affymetrix single-nucleotide-polymorphism genotyping microarrays. Am J Hum Genet 2007;81:114–26.

62. Imai Y, Strohmeyer TG, Fleischhacker M, Slamon DJ, Koeffler HP. p53 mutations and MDM-2 amplification in renal cell cancers. Mod Pathol 1994;7:766–70.

63. Mori N, Morosetti R, Lee S, et al. Allelotype analysis in the evolution of chronic myelocytic leukemia. Blood 1997;90:2010–4.

Frequent genomic abnormalities in acute myeloid leukemia/myelodysplastic syndrome with normal karyotype

Tadayuki Akagi,[1#] Seishi Ogawa,[2,3,4] Martin Dugas,[5] Norihiko Kawamata,[1] Go Yamamoto,[2] Yasuhito Nannya,[2] Masashi Sanada,[3,4] Carl W. Miller,[1] Amanda Yung,[1] Susanne Schnittger,[6] Torsten Haferlach,[6] Claudia Haferlach,[6] and H. Phillip Koeffler[1]

[1]Division of Hematology and Oncology, Cedars-Sinai Medical Center, UCLA School of Medicine, Los Angeles, CA, USA; [2]Department of Hematology and Oncology, and [3]Department of Cell Therapy and Transplantation Medicine and the 21st Century COE Program, Graduate School of Medicine, University of Tokyo, Tokyo, Japan; [4]Core Research for Evolutional Science and Technology, Japan Science and Technology Agency, Tokyo, Japan; [5]Department of Medical Informatics and Biomathematics, University of Munster, Munster, Germany; [6]MLL Munich Leukemia Laboratory, Munich, Germany

ABSTRACT

Background

Acute myeloid leukemia is a clonal hematopoietic malignant disease; about 45-50% of cases do not have detectable chromosomal abnormalities. Here, we identified hidden genomic alterations and novel disease-related regions in normal karyotype acute myeloid leukemia/myelodysplastic syndrome samples.

Design and Methods

Thirty-eight normal karyotype acute myeloid leukemia/myelodysplastic syndrome samples were analyzed with high-density single-nucleotide polymorphism microarray using a new algorithm: allele-specific copy-number analysis using anonymous references (AsCNAR). Expression of mRNA in these samples was determined by mRNA microarray analysis.

Results

Eighteen samples (49%) showed either one or more genomic abnormalities including duplication, deletion and copy-number neutral loss of heterozygosity. Importantly, 12 patients (32%) had copy-number neutral loss of heterozygosity, causing duplication of either mutant *FLT3* (2 cases), *JAK2* (1 case) or *AML1/RUNX1* (1 case); and each had loss of the normal allele. Nine patients (24%) had small copy-number changes (< 10 Mb) including deletions of *NF1*, *ETV6/TEL*, *CDKN2A* and *CDKN2B*. Interestingly, mRNA microarray analysis showed a relationship between chromosomal changes and mRNA expression levels: loss or gain of chromosomes led, respectively, to either a decrease or increase of mRNA expression of genes in the region.

Conclusions

This study suggests that at least one half of cases of normal karyotype acute myeloid leukemia/myelodysplastic syndrome have readily identifiable genomic abnormalities, as found by our analysis; the high frequency of copy-number neutral loss of heterozygosity is especially notable.

Key words: normal karyotype acute myeloid leukemia/myelodysplastic syndrome, SNP-chip, CNN-LOH.

Citation: Akagi T, Ogawa S, Dugas M, Kawamata N, Yamamoto G, Nannya Y, Sanada M, Miller CW, Yung A, Schnittger S, Haferlach T, Haferlach C, and Koeffler HP. Frequent genomic abnormalities in acute myeloid leukemia/myelodysplastic syndrome with normal karyotype. Haematologica 2009; Haematologica 2009; 94:213-223. doi:10.3324/haematol.13024

CH and HPK are co-last authors.

#Current address: Department of Stem Cell Biology, Graduate School of Medical Science, Kanazawa University. 13-1 Takara-machi, Kanazawa, Ishikawa 920-8640, Japan

Acknowledgments: we thank members of our laboratory for helpful discussions.

Funding: this work was supported by NIH grants as well as the Parker Hughes Fund. HPK is the holder of the Mark Goodson endowed Chair in Oncology Research and is a member of the Jonsson Cancer Center and the Molecular Biology Institute, UCLA. MD and TH are supported by the European Leukemia Network (funded by the 6th Framework Program of the European Community). The study is dedicated to the memory of David Golde, a mentor and friend.

Manuscript received March 5, 2008. Revised version arrived September 17, 2008. Manuscript accepted October 6, 2008.

Correspondence:
Tadayuki Akagi, Ph.D, Division of Hematology and Oncology, Cedars-Sinai Medical Center, UCLA School of Medicine 8700 Beverly Blvd, Los Angeles, CA90048, USA.
E-mail: tadayuki@staff.kanazawa-u.ac.jp

The online version of this article contains a supplementary appendix.

Introduction

Acute myeloid leukemia (AML) is a clonal malignant hematopoietic disease characterized by a block in differentiation, resulting in accumulation of immature myeloid cells.[1,2] Karyotypic analyses have revealed several frequent chromosomal translocations producing fusion genes associated with AML. The t(8;21)(q22;q22) translocation is one of these abnormal karyotypes, and this translocation produces *AML1-ETO* fusion products.[3,4] The *AML1-ETO* blocks hematopoietic differentiation and enhances self-renewal of human and murine hematopoietic stem cells.[5,6] The fusion product apparently binds to *AML1* target genes and represses their transcription.[5,6] The inv(16)(p13q22) or t(16;16)(p13;q22) produces the leukemogenic *CBFB-MYH11* fusion gene which blocks differentiation of hematopoietic stem cells by inhibiting the function of *AML1*.[7,8] Acute promyelocytic leukemia cells usually have t(15;17)(q22;q11-21) producing *PML-RARA* fusion products which also behave as a transcriptional repressor.[9,10] Other frequent translocations include t(9;11), t(6;11), inv(3)/t(3;3) and t(6;9).[11] Trisomy 8, 11, 13, 21 and 22, and deletion of chromosome 5/5q, 7/7q, 17/17p and 20/20q also occur moderately frequently.[2,11,12] About 45-50% of AML patients have no detectable chromosomal abnormalities.[13,14] In general, these individuals with a normal karyotype in their leukemic cells show an intermediate prognosis.[13,14]

Besides chromosomal abnormalities, the leukemic cells can have a variety of mutations involving individual genes. Activating mutations of the receptor tyrosine kinase, FMS-like tyrosine kinase 3 (*FLT3*) occur in about 30% AML patients; two major mutant forms occur: an internal tandem duplication (ITD) or a point mutation in the tyrosine kinase domain (TKD).[15] Activating mutations at codon 12, 13 or 61 of either the *NRAS* or *KRAS* occur in 25% and 15% of AML patients, respectively.[1,16] About 10-15% of AML samples have inactivating mutations of C/EBPα whose wild-type function is to enhance differentiation.[17,18] Nucleophosmin1 (NPM1) is mutated in 50-60% of AML samples with normal karyotype.[18,19] This protein has an important role in ribosome biogenesis, including nuclear export of ribosomal proteins. Mutant NPM1 has an aberrant nuclear export signal and remains localized in the cytoplasm.[20]

Single-nucleotide polymorphism microarray (SNP-chip) analysis is a new technique to examine the genome including any copy-number changes and loss of heterozygosity (LOH).[21-23] Importantly, SNP-chip analysis can reveal cryptic abnormalities such as a small copy-number changes (< 10 Mb) or copy-number neutral loss of heterozygosity [CNN-LOH, also called uniparental disomy (UPD)] that cannot be detected by karyotype analysis. In addition, comparative genomic hybridization cannot detect CNN-LOH. SNP-chip analysis has been used in chronic lymphocytic leukemia,[24,25] childhood acute lymphoblastic leukemia,[26,27] juvenile myelomonocytic leukemia,[28] follicular lymphoma,[29] multiple myeloma,[30] and AML.[31,32,50-54]

In the present study, we identified hidden abnormalities and novel disease-related genomic regions using 250 K SNP-chip analysis in samples from patients with normal karyotype AML/myelodysplastic syndrome (MDS). The use of CNAG (copy-number analysis for Affymetrix GeneChips) program[21] and a new algorithm AsCNAR (allele-specific copy-number analysis using anonymous references)[23] provided a highly sensitive technique to detect CNN-LOH, as well as, copy-number changes in AML/MDS genomes.

Design and Methods

Patients' samples

Samples from 30 anonymized patients with normal karyotype AML and 8 anonymized patients with normal karyotype MDS (age, 33-88 years; median, 62 years) were examined. These samples were isolated from bone marrow at diagnosis. The patients' age, gender, diagnosis, white blood cell count (WBC), karyotype and additional mutations of *FLT3* and *NPM1* are summarized in Table 1. This study was approved by Cedars-Sinai Medical Center (IRB number 4485).

High-density SNP-chip analysis

Genomic DNA was isolated from AML/MDS cells, and the DNA was subjected to GeneChip Human mapping 250 K array NspI microarray (SNP-chip, Affymetrix, Santa Clara, CA, USA) as described previously.[21,23] Hybridization, washing and signal detection were performed on GeneChip Fluidics Station 400 and GeneChip scanner 3000 according to the manufacturer's protocols (Affymetrix). Microarray data were analyzed for determination of both total and allelic-specific copy-number using the CNAG program as previously described[21,23] with minor modifications; the status of copy-numbers as well as CNN-LOH at each SNP was inferred using the algorithms based on hidden Markov models.[21,23] GNAGraph software was used for clustering of AML samples with regards to their copy-number changes, as well as CNN-LOH.[27] Size, position and location of genes were identified with UCSC Genome Browser *http://genome.ucsc.edu*. Copy-number changes, including duplication and deletion, were identified by allele-specific CNAG software.[25,27] These copy-number changes include copy-number variant and physiological deletion at the immunoglobulin and T-cell receptor genes. Copy-number variants as described previously at *http://projects.tcag.ca/variation* and physiological deletions were eliminated manually, and other regions detected by allele-specific CNAG software are listed on Table 4.

Fluorescence in situ hybridization analysis

Bone marrow samples from AML patients were used for interphase fluorescence *in situ* hybridization (FISH) analysis. The FISH studies were performed using the following probes: D5S721 (5p15.2), D5S23 (5p15.2), D7Z1 (centromere of chromosome 7), ABL (9q34.12), EGR1 (5q31.2), D7S486 (7q31), TP53 (17p13.1), D8Z2 (centromere of chromosome 8), AML1 (21q22.12) and BCR (22q11.23) (ABBOTT/VYSIS, Des Plaines, IL, USA). Probes for the 12p13 region [fluorescein-labeled ETV6-

downstream region (483 kb-length) and Texas-red-labeled ETV6-upstream region (264 kb-length)] were used for FISH analysis in case #5. The ETV6 probes were obtained from ABBOTT/VYSIS.

Determination of SNP sequences, JAK2, FLT3, NPM1, and AML1/RUNX1 mutations, and other target genes in cases of CNN-LOH

To determine the SNP sequences, (SNP identities are rs7747259, rs1122637, rs9505293, rs6934027, rs280153 and rs191986) in case #38 chromosome 6p region, the genomic region of each SNP site was amplified by genomic polymerase chain reaction (PCR) using specific primers. For determination of *JAK2* V617F mutation in case #20, genomic PCR was performed with specific primers. PCR products were purified and sequenced. The sequences of the primers are shown in *Online Supplementary Tables S1 and S2*. To determine the *FLT3*-ITD mutation, the PCR reaction was performed with specific primers, and the PCR products were separated on a 2.0% agarose gel stained with ethidium bromide as described previously.[34,35] Mutations at exon 12 of the *NPM1* gene were determined using a melting curve-based LightCycler assay (Roche Diagnostics, Mannheim, Germany).[36] Denaturing high-performance liquid chromatography analysis was performed to determine the *AML1/RUNX1* mutation in case #17 as described previously.[37] Alterations of several tyrosine kinase genes including *FGR* (case #3 and #23), *DDR1* (case #2 and 38), *TYK2* (case #2), *MATK* (case #2), *FER* (case #8) and *FGFR4* (case #8) were determined by either nucleotide sequencing of their exons and/or band-shifts of PCR products of exons after their electrophoresis and visualization on a gel (single strand conformation polymorphism), as described previously[38] with minor modifications. The PCR reaction contained genomic DNA, 500 nM of each of the primers, 200 nM of each of the dNTP, 0.5 units of Taq DNA polymerase and 3 μCi [α-32P] dCTP in 20 μL PCR products were diluted 10-fold in the loading buffer (10 mM NaOH, 95% formamide, and 0.05% of both bromophenol blue and xylene cyanol). After denaturation at 94°C for 5 min, 2 mL of the samples were loaded onto a 6% non-denaturating polyacrylamide mutation detection enhancement gel (Bioproducts, Rockland, ME, USA) with 10% (v/v) glycerol and separated at 300 V for 20 h. The gel was dried and subjected to autoradiography.

Table 1. Baseline clinical characteristics of 38 cases of normal karyotype acute myeloid leukemia/myelodysplastic syndrome.

Group	Case #	Gender	Age	Type	WBC x10⁹/L	*FLT3*	*NPM1*	Karyotype
A	29	M	49	AML M0	13.8	–	–	46,XY
	1	F	33	AML M1	3.5	–	–	46,XX
	14	M	43	AML M1	27.9	–	–	46,XY
	15	F	67	AML M1	365	–	+	46,XX
	6	M	66	AML M2	2.5	–	–	46,XY
	24	M	88	AML M2	6.3	–	–	46,XY
	25	F	61	AML M2	11.9	–	+	46,XX
	33	F	60	AML M2	24.5	+	+	46,XX
	44	M	65	AML M2	62.8	–	–	46,XY
	18	F	43	AML M4	43.1	–	+	46,XX
	19	M	37	AML M4	209	–	+	46,XY
	32	M	45	AML M4	9.5	–	+	46,XY
	34	F	80	AML M4	71.1	+	–	46,XX
	31	F	45	AML M5b	12.7	+	+	46,XX
	16	F	77	MDS RA	5.3	–	–	46,XX
	35	F	68	MDS CMML-1	5.6	–	–	46,XX
	36	F	69	MDS RAEB-1	4.6	–	–	46,XX
	39	F	74	MDS RAEB-1[1]	5.4	–	–	46,XX
	42	F	79	MDS	3.2	–	–	46,XX
B	10	F	49	AML M1	17.0	+	–	46,XX
	4	M	76	AML M2	2.3	–	–	46,XY
	5	F	67	AML M2	1.1	–	–	46,XX
	8	F	75	AML M2	1.8	–	–	46,XX
	9	M	65	AML M2	48.3	–	–	46,XY
	17	M	78	AML M2	1.1	–	–	46,XY
	20	F	65	AML M2	34.3	–	–	46,XX
	23	M	69	AML M2	2.0	–	+	46,XY
	26	M	36	AML M2	14.2	–	+	46,XY
	2	F	71	AML M4	1.9	–	+	46,XX
	7	F	85	AML M4	2.4	–	–	46,XX
	21	F	38	AML M4	37.6	+	+	46,XX
	38	M	53	AML M4	40	+	+	46,XY
	3	F	67	AML M5b	56	+	+	46,XX
	37	F	65	AML M5b	72.8	+	+	46,XX
	12	M	69	MDS RA	11.5	–	–	46,XY
	41	M	77	MDS RA[1]	7.1	–	–	46,XY
	13	F	54	MDS RAEB-2	–	–	–	46,XX
	11	F	60	t-AML M2	1.7	–	–	46,XX

t-AML: therapy-related AML; RA: refractory anemia; RAEB-1 or -2: refractory anemia with excess blasts subtype-1 or -2; CMML: chronic myelomonocytic leukemia; [1]new WHO classification.

Quantitative real-time polymerase chain reaction

Gene-dosages of chromosome 6p24.3 in case #38, and the *MYC* and *CDKN2A* genes in case #20 were determined by quantitative real-time PCR (iCycler, Bio-Rad, Hercules, CA, USA) using Sybr Green. To determine the relative gene dosage of each sample, the chromosome 2p21 region was measured as a control.[37] The copy-number of the 2p21 region was normal, as determined by SNP-chip analysis, in these samples. The delta threshold cycle value (ΔCt) was calculated from the given Ct value by the formula ΔCt = (Ct sample - Ct control). The fold change was calculated as $2^{-\Delta Ct}$. Primer sequences are shown in *Online Supplementary Table S2*.

Gene expression microarray analysis

Total RNA was isolated from AML/MDS cells and processed according to Affymetrix guidelines for analysis with HGU133 Plus 2.0 microarrays. Data were analyzed with R version 2.5.0 using Bioconductor version 2.0.[39] Data were normalized using the robust multi-array average procedure.[39] Since most regions that showed chromosomal abnormalities were not recurring, we were not able to compare individual genes across samples with statistical tests. To assess plausibility of large deletions and amplifications, we subtracted

from each gene (in the respective region) mean expression of this gene in other cases: case #11 was compared with 37 normal karyotype AML/MDS cases; and cases #20, #4 and #5 were compared with other normal karyotype AML/MDS samples. We then calculated a mean expression difference for each region and considered a value below zero to be consistent with deletion and a value above zero to be consistent with amplification.

Results

Proof of principal

To identify hidden abnormalities in AML/MDS with a normal karyotype, 37 samples were analyzed by 250K SNP-chip microarray. One additional case (case #11) had only 13 metaphases and chromosomal abnormalities were not detected on karyotypic analysis; this sample did, however, have numerous genetic abnormalities identified by SNP-chip including hemizygous deletions of 3p25.1-p24.3 (2.29 Mb), 3p24.2-p24.1 (3.96 Mb), 3p23-q12.1 (66.55 Mb), 5q11.2-q-terminal (124.89 Mb), 7q11.23-q36.1 (76.04 Mb), 7q36.2 (0.78 Mb), 11q23.3-q-terminal (18.24 Mb), 17p-terminal-q11.1 (22.48 Mb), and 17q11.2-q12 (4.42 Mb); duplications of 3p24.3 (2.14 Mb), 5p15.31 (1.83 Mb), and 5p14.3-q11.2 (35.53 Mb); and trisomy of chromosomes 8, 21 and 22 (Table 2). To confirm these SNP-chip results, we performed extensive FISH analysis. The number of signals for probes D5S721 (5p15.2), D5S23 (5p15.2), D7Z1 (centromere of chromosome 7) and ABL (9q34.12) was two, and SNP-chip analysis also showed normal copy number (2n) consistent with the SNP-chip data. The EGR1 (5q31.2), D7S486 (7q31) and TP53 (17p13.1) probes revealed one signal; and these regions also showed hemizygous deletion (1n) by SNP-chip analysis. D8Z2 (centromere of chromosome 8), AML1 (21q22.12) and BCR (22q11.23) probes showed three or four signals, and SNP-chip analysis also indicated trisomy (3n) of these chromosomes. Chromosome 9 was normal by both SNP-chip and FISH analyses. As summarized in *Online Supplementary Table S3*, the results of SNP-chip and FISH analyses were completely congruent. Taken together, these results suggest that SNP-chip analysis reflected the genomic changes.

SNP-chip analysis in 37 normal karyotype acute myeloid leukemia/myelodysplastic syndrome samples

SNP-chip analysis of samples from 37 patients with normal karyotype AML/MDS revealed several genomic copy-number changes, as well as CNN-LOH. Nineteen patients (51%) had a normal genome by SNP-chip analysis (group A). In contrast, 18 patients (49%) had one or more genomic abnormalities (group B) (Figure 1). Deletions and/or duplications were found in nine patients (24%). Twelve patients (32%) had CNN-LOH. In group B, 14 cases (78% of the 18 samples) had only one genomic change; one case (6%) had two genomic abnormalities (case #5); two cases (11%) had three changes (case #2 and #4) and one case (5%) had four genomic alterations (case #20).

We also compared the relationship between the genomic changes and the French-American British classification of the 15 AML and 3 MDS samples in group B. In the AML samples, 11 cases had CNN-LOH, three cases had a duplication and seven cases had a deletion. The one AML M1 sample (case #10) had CNN-LOH; and the two AML M5b samples (cases #3 and #37) had CNN-LOH in their chromosomes. In the four AML M4 samples, cases #38, #21 and #2 had CNN-LOH, and cases #2 and #7 had a small deletion. In eight AML M2 samples, five (cases #4, #8, #17, #20, and #23) had CNN-LOH, three (cases #4, #5 and #20) had a duplication, and five (cases # 4, #5, #9, #20 and #26) had a deletion. In the three MDS samples, one sample (case #12) had CNN-LOH, and two samples (cases #13 and #41) had a deletion (Figure 1, Tables 3 and 4). Taken together, these results show that the patients who were categorized as having normal karyotype AML/MDS had easily recognizable deletions, duplications and/or CNN-LOH of their genome.

Table 2. Copy-number changes in case #11 detected by SNP-chip analysis.

Chromosome	Location	Physical localization		Size (Mb)	Status
		Proximal	Distal		
3	3p25.1-p24.3	16,389,202	18,675,075	2.29	Del
	3p24.3	19,589,378	21,731,557	2.14	Dup
	3p24.2-p24.1	24,881,910	28,844,599	3.96	Del
	3p23-q12.1	33,278,003	99,828,897	66.55	Del
5	5p15.31	7,616,335	9,443,217	1.83	Dup
	5p14.3-q11.2	18,603,838	54,129,781	35.53	Dup
	5q11.2-q-ter.	55,738,905	180,629,495	124.89	Del
7	7q11.23-q36.1	71,659,926	147,695,696	76.04	Del
	7q36.2	152,027,450	152,806,031	0.78	Del
8	Trisomy				
11	11q23.3-q-ter.	116,202,097	134,439,182	18.24	Del
17	17p-ter.-q11.1	18,901	22,494,871	22.48	Del
	17q11.2-q12	25,499,505	29,918,396	4.42	Del
21	Trisomy				
22	Trisomy				

AML case #11 had numerous genetic abnormalities. Location and size (Mb) were obtained from UCSC Genome Browser. Copy-number changes previously described as copy-number variant were excluded. Del: deletion; Dup: duplication; ter: terminal.

Chromosomal region and candidate genes in CNN-LOH detected by SNP-chip analysis

Previous studies demonstrated CNN-LOH in AML samples at a frequency of 15-20%.[31,32,50,51,53,54] Our analysis with AsCNAR (allele-specific copy-number analysis using anonymous references) revealed CNN-LOH in 32% of the AML/MDS samples with a normal karyotype; the median size of the CNN-LOH was 30.91 Mb (range, 11.76 Mb–103.77 Mb). We found some cases with a recurrent region of CNN-LOH. Cases #3 and #23 had CNN-LOH on 1p, and the common region of CNN-LOH (30.85 Mb) included the tyrosine kinase genes (*FGR*, *EPHA2* and *EPHB2*) and an imprinted tumor suppressor gene *TP73* (Table 3). Cases #2 and #38 had CNN-LOH on 6p and the common region of CNN-LOH (30.97 Mb) contained the tyrosine kinase gene *DDR1* (Table 3). Cases #4 and #37 had CNN-LOH on 8q and the common region of CNN-LOH (11.76 Mb) contained the tyrosine kinase gene *PTK* (Table 3). CNN-LOH of the

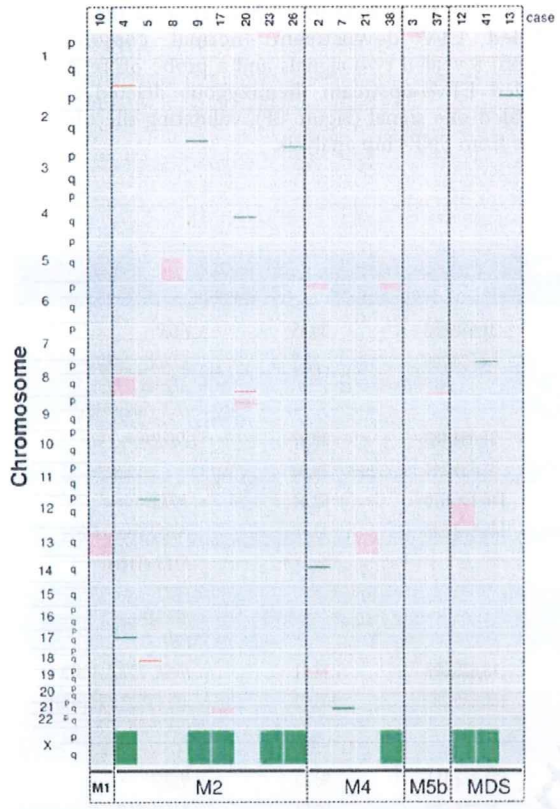

Figure 1. Genomic DNA of 37 acute myeloid leukemia samples with normal karyotype were subjected to SNP-chip analysis; genomic abnormalities are summarized. Pink, green and red bars/boxes indicate CNN-LOH, deletion and duplication, respectively. Nineteen patients (51%) showed no detectable genomic abnormalities (*data not shown*), whereas 18 patients (49%) had one or more genomic abnormalities. Deletion or duplication was found in nine patients (24%), and CNN-LOH occurred in 12 patients (32%). Chromosomal location, size and genes are shown in Tables 3 and 4.

whole region of 13q was found in cases #10 and #21; this region contains the *FLT3*, *FLT1*, *BRCA2* and *RB1* genes (Table 3).

Cases #2, #8, #12, #17 and #20 had CNN-LOH on 19p (13.41 Mb), 5q (103.77 Mb), 12q (96.23 Mb), 21q (29.54 Mb) and 9p (43.96 Mb), respectively. Although these regions of CNN-LOH occurred in only one case each, several interesting genes were found in the region, including *INSR*, *TYK2*, and *MATK* (case #2); *APC*, *FER*, *FMS/FLT4*, *PDGFRB*, *ITK* and *FGFR4* (case #8), *AML1/RUNX1* (case #17), and *JAK2* and *TEK* (case #20) (Table 3).

Interestingly, cases #10 and #21 had a *FLT3*-ITD gene mutation (Table 3); case #17 had an *AML1/RUNX1* frameshift caused by a deletion of cytosine at nucleotide 211 (Table 3). Sequencing of *JAK2* in case #20 showed a homozygous canonical *JAK2* mutation [V617F (GTC → TTC)] (Table 3). Each of these mutations occurred at a CNN-LOH. The data suggest that removal of a normal allele and duplication of the mutated allele is favored by the cancer cells.

Validation of copy number-neutral loss of heterozygosity

To validate CNN-LOH, we determined SNP sequences and gene-dosage in a CNN-LOH region using case #38 (Figure 2). If a chromosome has LOH, the nucleotide at the SNP site should not be heterozygous, but should be homozygous. We, therefore, examined six independent SNP sites in case #38 on the chromosome 6p region of CNN-LOH including rs7747259, rs1122637, rs9505293, rs6934027, rs280153 and rs191986. All six SNP sites showed only a single nucleotide; no SNP sites showed heterozygosity (Figure 2B). Each one of these sites is heterozygous in the general population at a frequency varying between 25% and 42% (*Entrez SNP database, http://www.ncbi.nlm.nih.gov/sites/entrez?db=snp*). These results strongly suggest that this region has LOH.

Next, we determined gene-dosage of the region to exclude the possibility of hemizygous deletion. The gene-dosage of 6p24.3 in case #38 was compared to that of normal genomic DNA using quantitative genomic real-time PCR by comparing the ratio between 6p24.3 and the reference genomic DNA, 2p21. As shown in Figure 2C, the amount of DNA at this site for case #38 was almost the same as that for normal genomic DNA, indicating that this region is not deleted. Taken together, our sequence data and gene dosage study validated the results of our SNP-chip analysis, clearly showing CNN-LOH at 6p24.3.

Chromosomal regions of copy-number change detected by SNP-chip analysis

Nine patients (24%) had small copy-number changes including deletions and/or duplications; the median size of the duplications and deletions was 0.3 Mb (range, 0.09–4.33 Mb) and 0.625 Mb (range, 0.11–5.87 Mb), respectively. As shown in Table 4, hemizygous deletions were found at 14q21.2 (0.3 Mb, case #2), 17q11.2 (2.7 Mb, case #4), 12p13.31 - p13.2 (2.91 Mb, case #5), 21q21.2 (0.44 Mb, case #7), 2q36.2 (0.41 Mb, case #9), 2p23.1 (0.56 Mb, case #13), 4q24 (1.08 Mb, case #20), 9p21.3 - p21.2 (5.87 Mb, case #20), 3p26.3 (0.69 Mb, case #26), and 8p23.2 (0.11 Mb, case #41). Cases #4, #5 and #20 had duplication at 1q43 (0.09 Mb), 18q21.2 (0.3 Mb), and 8q24.13 - q24.21 (4.33 Mb), respectively. These regions contain well-known oncogenes and tumor suppressor genes (Table 4). The tumor suppressor genes, *NF1* and *CDKN2A/CDKN2B*, and the transcription factor, *ETV6/TEL* were deleted in cases #4, #20 and #5, respectively; and the oncogene *MYC* was duplicated in case #20.

Validation of copy-number changes

Next, we validated copy-number changes in cases #20 and #5 using different techniques. Case #20 had duplication at 8q24.13 - q24.21 (Figure 3A) and hemizygous deletion at 9p21.3 - p21.2 (Figure 3B); these regions contain the oncogene *MYC* and the tumor suppressor genes *CDKN2A* and *CDKN2B*, respectively. Relative gene-dosages of the *MYC* and *CDKN2A* genes were examined by quantitative genomic real-time PCR with the chromosome 2p21 region as a control. The

level of the *MYC* gene was about 2-fold higher while the level of the *CDKN2A* gene was approximately 10-fold lower compared with normal genomic DNA (Figures 3C and D).

Chromosome 12p13.31 - p13.2 was deleted in case #5; this region contains the transcription factor *ETV6/TEL* (Figure 3E). FISH analysis with a probe of fluorescein-labeled ETV6-downstream (normal copy-number region) revealed two signals and a probe of Texas-red-labeled ETV6-upstream (hemizygous deleted region) revealed one signal (Figure 3F), validating the observations from SNP-chip analysis.

Table 3. Chromosomal regions identified as CNN-LOH.

Case*	FAB	Location	Physical localization Proximal	Distal	Size (Mb)	Genes
3	AML M5b	1p-ter.-p35.2	825,852	31,679,683	30.85	*FGR*
23	AML M2	1p-ter.-p35.1	825,852	33,526,200	32.7	*EPHA2, EPHB2 EPHA8, TP73 LCK* (only #23)
2	AML M4	6p-ter. - p21.3	3119,769	31,094,483	30.97	*DDR1*
38	AML M4	6p-ter. - p21.3	1119,769	33,781,344	33.66	
4	AML M2	8q12.3 - q-ter.	64,069,382	146,106,670	82.04	*PTK2*
37	AML M5b	8q24.22 - q-ter.	134,507,898	146,263,538	11.76	*NBS1* (only #4)
10	AML M1	Whole 13q				*FLT3* (ITD)
21	AML M4	Whole 13q				*FLT1 BRCA2 RB1*
2	AML M4	19p-ter. - p13.13	212,033	13,625,099	13.41	*INSR, TYK2, MATK*
8	AML M2	5q13.3 - q-ter	76,761,338	180,536,297	103.77	*APC, FER, FMS/FLT4 PDGFRB, ITK, FGFR4, NPM1*
12	MDS RA	12q11 - q-ter.	36,144,018	132,377,151	96.23	*HER3*
17	AML M2	21q21.1 - q-ter.	17,346,621	46,885,639	29.54	*AML1/RUNX1* (delC211, frameshift)
20	AML M2	9p-ter. - p21.3 9p21.2 - q21.11	140,524 27,142,682	21,047,062 44,108,554	20.91 16.97	*JAK2* (V617F) *TEK*

Twelve patients (32%) had CNN-LOH. Physical localization, size (Mb), and genes were obtained from UCSC Genome Browser. Note: Cases #10 and #21 had a mutant form of FLT3-internal tandem repeat [FLT3 (ITD)]. Case #20 had a mutant JAK2 (JAK2V617F) *which is constitutively active, and case #17 had a deletion of cytosine at nucleotide 211 of* AML1/RUNX1, *resulting in a frameshift. *, Known tyrosine kinase and tumor suppressor genes are shown.*

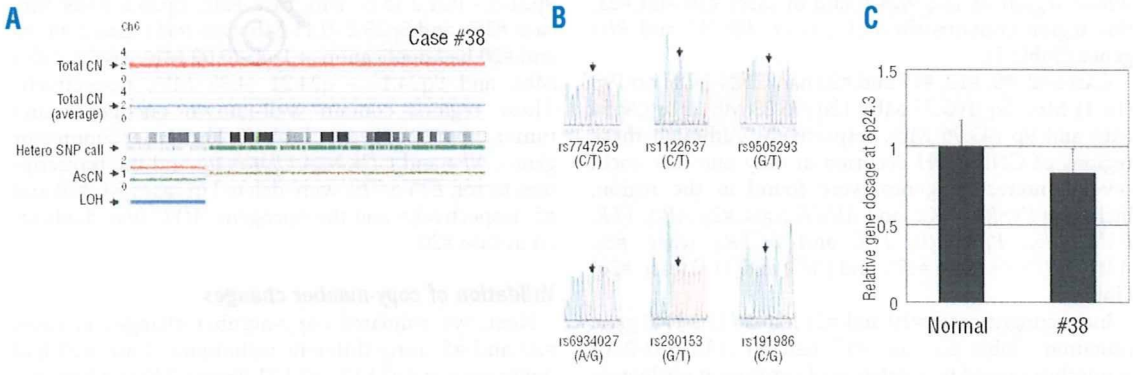

Figure 2. Validation of CNN-LOH (**A**) Region of CNN-LOH in chromosome 6 of case #38. Red dots represent SNP sites as probes and indicate total copy-number. The blue line represents an average of copy-number and shows gene dosage. Green bars represents heterozygous (hetero) SNP calls. Red and green lines show allele-specific copy-number (AsCN). Blue bars indicate LOH detected by heterozygous SNP calls. (**B**) Determination of SNP sequences in the 6p region. Six independent SNP sites were sequenced. All six SNP sites contained only a single nucleotide; no SNP site displayed heterozygosity. Results are consistent with CNN-LOH. (**C**) Determination of gene-dosage in the 6p region. Gene-dosage of 6p24.3 (CNN-LOH region) in case #38 is compared to that in normal genomic DNA using quantitative genomic real-time PCR. Levels of the gene-dosage were determined as a ratio between 6p24.3 and the reference genomic DNA, 2p21.

Table 4. Chromosomal location of small copy-number changes.

Case#	Type	Location	Physical localization Proximal	Physical localization Distal	Size (Mb)	Status	Gene*
4	AML M2	1q43	235,009,590	235,101,866	0.09	Dup	
		17q11.2	25,002,820	27,705,467	2.7	Del	*NF1*
5	AML M2	12p13.31-p13.2	9,312,096	12,218,922	2.91	Del	*ETV6/TEL*
		18q21.2	49,053,520	49,357,887	0.3	Dup	
9	AML M2	2q36.2	225,014,233	225,424,075	0.41	Del	
20	AML M2	4q24	105,640,274	106,723,813	1.08	Del	
		8q24.13 - q24.21	126,445,881	130,777,342	4.33	Dup	*MYC*
		9p21.3 - p21.2	21,063,692	26,935,976	5.87	Del	*CDKN2A, CDKN2B*
26	AML M2	3p26.3	1,221,075	1,911,873	0.69	Del	
2	AML M4	14q21.2	45,915,366	46,216,073	0.3	Del	
7	AML M4	21q21.2	23,126,095	23,566,855	0.44	Del	
41	MDS RA*	8p23.2	3,483,631	3,589,278	0.11	Del	
13	MDS RAEB-2	2p23.1	30,659,972	31,220,245	0.56	Del	

*Nine patients (24%) had deletion and/or duplication. Location, size (Mb), and genes were obtained from UCSC Genome Browser. Copy-number changes previously described as copy-number variant were excluded. Del; deletion, Dup; duplication. *Known oncogenes and tumor suppressor genes are shown.*

Relationship between genomic abnormalities and mutant genes within the region

In our normal karyotype AML/MDS samples, eight cases (21%) had *FLT3*-ITD and 14 cases (37%) had a *NPM1* mutation (Table 1). We compared genomic abnormalities, and *FLT3*-ITD and *NPM1* mutations (*Online Supplementary Table S4*). Both *FLT3*-ITD and *NPM1* were mutated in two samples in group A (11%) and four cases in group B (22%). A single mutation of *FLT3*-ITD was found in one sample in group A (5%) and one case in group B (6%); a single mutation of *NPM1* occurred in five samples in group A (26%) and three samples in group B (17%). These mutations were, therefore, dispersed between both groups A and B

Relationship between genomic abnormalities and gene expression

We compared genomic abnormalities and gene expression. mRNA microarray analysis was done on all samples.[49] First, the level of mRNA expression in case #11 was compared with that in 37 normal karyotype AML samples. Affymetrix microarray analysis showed decreased average gene expression in the deleted regions and increased gene expression for regions with trisomy: the difference of average expression of genes located on deleted regions of chromosomes 5, 7, 17, as well as, trisomy 8, 21 and 22 were -0.21±0.01, -0.16 ±0.013, -0.27±0.018, +0.21±0.012, +0.22±0.022 and +0.15±0.013 (mean difference ± standard error), respectively (Figure 4A and *data not shown*).

Next, we examined the relationship between small copy-number changes and mRNA expression levels in the region. For this analysis, we chose deleted regions on chromosome 9 in case #20 (Figure 3B), chromosome 17 in case #4 (Table 4) and chromosome 12 in case #5 (Figure 3E). The differences in mean expression of genes located in deleted regions of chromosomes 9 (case #20), 17 (case #4), and 12 (case #5) were -0.15±0.07, -0.37±0.07, and -0.23±0.051 (mean difference ± standard error), respectively (Figure 4B). These results showed that large and small copy-number changes led to alterations of mRNA expression. In addition, the difference in mean expression of genes located in the CNN-LOH regions of each sample was comparable to that in normal copy-number samples, suggesting that CNN-LOH does not contribute to aberrant levels of gene expression (*data not shown*).

Discussion

Our genome-wide SNP-chip analysis of normal karyotype AML/MDS showed that 49% of these samples had one or more genomic abnormalities including deletions, duplications and CNN-LOH. Previous studies demonstrated that CNN-LOH occurs in AML samples at a frequency of 15-20%.[31,32,50,51,53,54] Of interest, about 40% of cases of relapsed of AML had CNN-LOH.[52] In our analysis, 32% of samples had CNN-LOH, and these regions of CNN-LOH contain several tyrosine kinase and tumor suppressor genes that may be candidate target genes in normal karyotype AML/MDS. In fact, the *FLT3*-ITD (13q12.2), *JAK2* V617F (9p24.1) and deletion of a cytosine at nucleotide 211 of *AML1/RUNX1* (21q22.12) occurred in areas of CNN-LOH resulting in duplication of these mutant genes and loss of the normal allele. A prior paradigm was that CNN-LOH marked the location of a mutated tumor suppressor gene, but it is clear that CNN-LOH can also be a signpost of an activated (mutated) oncogene. Of note, several CNN-LOH, including a region on chromosome 1p (cases #3 and #23), 6p (cases #2 and #38), 8q (cases #4 and 37) and 13q (cases #10 and #21), occurred in more than one sample. In addition, CNN-LOH of these regions, as well as several other unique CNN-LOH regions in our cohort, were also found in other stud-

ies.[50,51,58] Although these alterations are not frequent, shared regions of CNN-LOH clearly highlight their importance. These findings prompted us to screen genes located in CNN-LOH regions. We focused on tyrosine kinase genes including *FGR* (cases #3 and #23), *DDR1* (cases #2 and #38), *TYK2* (case #2), *MATK* (case #2), *FER* (case #8) and *FGFR4* (case #8), and either determined their exon nucleotide sequences or looked for single strand conformation polymorphism band-shifts of PCR products of the exons. However, these genes did not have detectable mutations (*data not shown*). Nevertheless, we believe that these CNN-LOH, as well as deletions and duplications, are acquired somatic mutations. We examined these regions for known copy-number polymorphisms (web site, *http://projects.tcag.ca/variation*) and found none. Also previously, we compared SNP-chip data between matched samples of acute promyelocytic leukemia and normal genomic DNA from the same individual (Akagi *et al.*, unpublished data) and found that CNN-LOH occurred only in the leukemia samples but not in the corresponding germline DNA. Furthermore, SNP-chip analysis easily detected a deletion on chromosome 3 (0.69 Mb) in case #28 in the AML sample which was not present in the remission bone marrow sample from the same individual (*Online Supplementary Figure S1*). Taken together, these findings suggest that the alterations detected by SNP-chip analysis are somatic mutations.

We also found small copy-number changes in some cases. Several features of case #20 are worthy of comment. The *MYC* gene was duplicated, and the *CDKN2A* (*p16/INK4A* and *p14/ARF*) and *CDKN2B* (*p15/INK4B*) genes were hemizygously deleted. Prominent expression of C-MYC protein is associated with stimulation of p14/ARF which inactivates MDM2, producing greater levels of p53 resulting in either apoptosis or slowing of cell growth which allows for DNA repair.[41,42] However, when the *p14/ARF* gene is deleted, C-MYC has an unfettered ability to stimulate growth of the cells. Case #20 had this constellation of changes. Furthermore, this individual had a homozygous *JAK2* mutation. *JAK2* is mutated (codon 617, valine changed to phenylalanine) and constitutively active in nearly 100%, 50% and 30% of samples from patients with polycythemia vera, agnogenic myeloid metaplasia and essential thrombocythemia, respectively, as well as in 1-3% of AML cases.[43-48] We do not know the prior history of this individual.

Some of the deleted genes are of particular interest; first, the tumor suppressor gene *NF1* was deleted in case #4. Children with neurofibromatosis type-1 have inactivating mutations of the *NF1* and an increased risk of developing juvenile myelomonocytic leukemia,[46] and LOH at the *NF1* gene locus occurs in this form of leukemia and other cancers. A recent study showed that three of 103 T-ALL (3%) samples and two of 71 AML samples with *MLL* rearrangements (3%) had deletion of the *NF1* gene region; a mutation in the remaining *NF1* allele was found in three samples, suggesting that *NF1* inactivation might be involved in the development of leukemia. Second, concerning case #5 (deletion of *ETV6/TEL*), *ETV6/TEL* is a transcriptional repressor and is involved in various translocations associated with

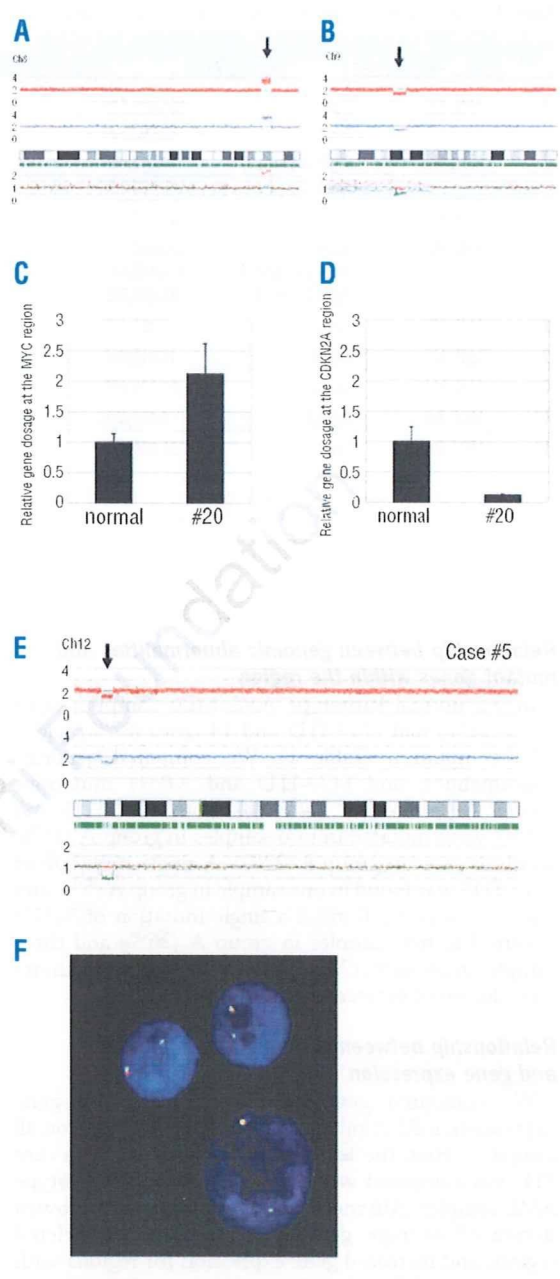

Figure 3. Validation of duplication and deletion: (**A**) Chromosome 8q24.13-q24.21 is duplicated. This region contains the oncogene *MYC*. (**B**) Chromosome 9p21.3 - p21.2 shows a deletion. The deleted region contains the tumor suppressor genes *CDKN2A* (*p16/INK4A* and *p14/ARF*) and *CDKN2B* (*p15/INK4B*). (**C**, **D**) Gene-dosages of the *MYC* gene (**C**) and the *CDKN2A* gene (**D**) region in case #20 are compared to normal genomic DNA by quantitative genomic real-time PCR. Levels of the gene-dosage are determined as a ratio between target gene and the reference genomic DNA, 2p21. (**E**) Case #5 had hemizygous deletion in chromosome 12p13.31-p13.2; this region contains the transcription factor *ETV6/TEL* gene. Physical localization and size are presented in Table 4. (**F**) FISH analysis of case #5 with probes for the *ETV6/TEL* region. Probes of fluorescein-labeled ETV6-downstream (normal region by SNP-chip analysis) and Texas-red-labeled ETV6-upstream (hemizygous deleted region by SNP-chip analysis) revealed one and two signals, respectively.